PL-TR-95-2115

THEATER ANALYSIS PROCEDURES (TAP) SYSTEM DEVELOPMENT: RESULTS FROM YEAR 1.

Thomas Nehrkorn
Ross N. Hoffman
Min Yin

DTIC
ELECTE
NOV 28 1995
S D
B

Atmospheric and Environmental Research, Inc.
840 Memorial Drive,
Cambridge, MA 02139

August 18, 1995
Scientific Report No. 1

19951124 008

Approved for public release; distribution unlimited

PHILLIPS LABORATORY
Directorate of Geophysics
AIR FORCE MATERIEL COMMAND
HANSCOM AIR FORCE BASE, MA 01731-3010

DTIC QUALITY INSPECTED 1

"This technical report has been reviewed and is approved for publication."

Donald C. Norquist

DONALD C. NORQUIST
Contract Manager

Donald A. Chisholm

DONALD A. CHISHOLM
Chief, Satellite Analysis and Weather Prediction Branch
Atmospheric Sciences Division

Robert A. McClatchey

ROBERT A. McCLATCHEY, Director
Atmospheric Sciences Division

This report has been reviewed by the ESC Public Affairs Office (PA) and is releasable to the National Technical Information Service (NTIS).

Qualified requestors may obtain additional copies from the Defense Technical Information Center (DTIC). All others should apply to the National Technical Information Service (NTIS).

If your address has changed, or if you wish to be removed from the mailing list, or if the addressee is no longer employed by your organization, please notify PL/IM, 29 Randolph Road, Hanscom AFB, MA 01731-3010. This will assist us in maintaining a current mailing list.

Do not return copies of this report unless contractual obligations or notices on a specific document requires that it be returned.

REPORT DOCUMENTATION PAGE

Form Approved
OMB No. 0704-0188

Public reporting burden for this collection of information is estimated to average 1 hour per response, including the time for reviewing instructions, searching existing data sources, gathering and maintaining the data needed, and completing and reviewing the collection of information. Send comments regarding this burden estimate or any other aspect of this collection of information, including suggestions for reducing this burden, to Washington Headquarters Services, Directorate for Information Operations and Reports, 1215 Jefferson Davis Highway, Suite 1204, Arlington, VA 22202-4302, and to the Office of Management and Budget, Paperwork Reduction Project (0704-0188), Washington, DC 20503.

1. AGENCY USE ONLY (Leave blank)	2. REPORT DATE	3. REPORT TYPE AND DATES COVERED
	18 August 1995	Scientific Report No.1

4. TITLE AND SUBTITLE

Theater Analysis Procedures (TAP) System Development: Results from Year 1.

5. FUNDING NUMBERS

F19628-94-C-0027
PE 63707F
PR 2688
TA G-V WUMA

6. AUTHOR(S)

Thomas Nehrkorn, Ross Hoffman, Min Yin

7. PERFORMING ORGANIZATION NAME(S) AND ADDRESS(ES)

Atmospheric and Environmental Research, Inc.
840 Memorial Drive
Cambridge, MA 02139

8. PERFORMING ORGANIZATION REPORT NUMBER

9. SPONSORING/MONITORING AGENCY NAME(S) AND ADDRESS(ES)

Phillips Laboratory
29 Randolph Road
Hanscom AFB MA 01731-3010
Contract Monitor: Don Norquist/GPAP

10. SPONSORING/MONITORING AGENCY REPORT NUMBER

PL-TR-95-2115

11. SUPPLEMENTARY NOTES

12a. DISTRIBUTION/AVAILABILITY STATEMENT

Approved for public release; distribution unlimited

12b. DISTRIBUTION CODE

13. ABSTRACT *(Maximum 200 words)*

This report describes the results of the first year of a 3-year project for development of a theater-scale meteorological analysis system based on the method of optimal interpolation. The TAP project primary objective is to develop robust analysis procedures to support the tactical user. These analysis procedures provide stable meteorological products for end users. The function of TAP is to combine background (*i.e.* a priori) information with observations of diverse type, quality, and density to produce analyses of meteorological fields. The status of the system design and prototyping is reviewed. Real data collected for system testing is described. The climatology and error statistics databases generated during the first year are described.

14. SUBJECT TERMS

Objective analysis, Optimal interpolation
Numerical weather prediction, Climatology

15. NUMBER OF PAGES

50

16. PRICE CODE

17. SECURITY CLASSIFICATION OF REPORT	18. SECURITY CLASSIFICATION OF THIS PAGE	19. SECURITY CLASSIFICATION OF ABSTRACT	20. LIMITATION OF ABSTRACT
Unclassified	Unclassified	Unclassified	SAR

Contents

Accession For
NTIS GRA&I ☑
DTIC TAB ☐
Unannounced ☐
Justification
By
Distribution/
Availability Codes
Dist | Avail and/or Special
A-1

1 Introduction

This report describes the progress made during the first year of the TAP (Theater-scale Analysis Procedure) project.

The TAP project primary objective is to develop robust analysis procedures to support the tactical user. These analysis procedures provide stable meteorological products for end users.

The function of TAP is to use the optimal interpolation technique to combine background (i.e. *a priori*) information with observations of diverse type, quality, and density to produce analyses of meteorological fields. The TAP analysis configurations are optimized to initialize NWP models and to provide input for Electro-optical decision aids (EOTDAs).

TAP is modular, and capable of utilizing a variety of background and data sources. This capability allows TAP to adapt to different theater meteorological support systems (TMSSs), run on different platforms and to satisfy different user requirements. TAP is configurable to a range of requirements, from first-in stand-alone capability to full Theater Weather Central (TWC) support.

In the nominal case, background fields for TAP are obtained from short-term forecasts of a global NWP model. This requires established communication links, and a set of representative forecast error statistics (standard deviations and correlations). If timely forecasts are not available, older, longer-range forecasts can be used instead, which requires the use of modified error statistics. Finally, if no usable forecast data exist, a climatological background is used.

During the first year of the project, work has proceeded along several separate fronts:

- System design, prototyping, and unit testing
- Data collection
- System testing
- Development of climatology database
- Development of statistics database

A preliminary system design was formulated, reviewed by internal and and external reviewers, and partially implemented. A working prototype system has been implemented which contains all the major elements of the final system, with placeholders for those components that have not been prototyped according to the system design. Code development and unit testing are proceeding within the framework of this prototype system. The details of the system design are not repeated here – they are provided in a separate contract deliverable. Preliminary results from this prototype system are shown in Section 5.

System testing by outside users using real data is scheduled for the end of the second project year. To support this testing, as well as our internal system tests, we have begun collection of real data over the Eastern United States. A description of the collection procedures, supporting software, and the cases selected so far is given in Section 2.

The climatology data required for the background have been collected and processed during the first year. This work is described in Section 3.

Finally, an extensive bibliography search was conducted to collect and select appropriate statistics for background and observation errors. A summary of the results of this work is given in Section 4.

2 Real-Data Tests

2.1 Data Sources and Collection Procedures

Real data for system tests have been collected from a variety of sources. The selection of the data sources was driven by the competing requirements of ease of access and ingest of the data on the one hand, and adequate geographical coverage and representation of different background and data types on the other. Conventional (surface, ship, buoy, and upper air) data are collected and decoded using the Family of Services database and associated software on the AIMS (Air Force Interactive Meteorological System) system located at the Phillips Laboratory and operated by AER personnel. Direct-readout satellite data are collected from the NOAA and DMSP polar orbiters, using the AIMS ground station equipment. The direct-readout satellite data cover only the area visible from the satellite while transmitting to the ground station, which is centered over the East Coast of the United States. Because of this restriction, conventional data are only collected between latitudes 15° N and 60° N, and longitudes 45° W and 105° W. In addition, decoded off-shore data are collected from the National Data Buoy Center (NDBC) operated by NOAA using Internet connections. A variety of gridded model forecast and analysis fields are obtained from the anonymous NCEP ftp-server. The gridded fields obtained from NCEP are all in GRIB format, and software has been assembled and/or written to decode these data, ingest them into Splus, and display them over map backgrounds. The software was tested by comparing the displayed fields with independently obtained maps of the same fields. The conventional data is decoded into ASCII tables which are easy to ingest into Splus. The satellite direct-readout data will be processed using software installed on the AIMS ground station. The TOVS export package for obtaining temperature and moisture retrievals from the NOAA polar orbiter data was recently installed at PL; permission was obtained to use this package for the TAP project, and decoding and ingest into Splus will commence in the coming months. Software for performing statistical retrievals of the DMSP polar orbiter data still needs to be installed.

2.2 Cases Collected

2.2.1 6-7 March 1995

Data have been collected for approximately a 24-hour period centered around 12 UTC 6 March 1995. The synoptic situation on that day was characterized by an upper-level short-wave passing through the Northeastern United States and Canada, embedded in a southwesterly upper-level flow. At the surface, this was accompanied by a weak low (central pressure around 1016 hPa) and rain over the Northeastern United States, snow over parts of Quebec and the Canadian Maritimes. Height analyses at 850 hPa are shown in Section 5. This case represents a typical moderate to weak winter/early spring storm over the Northeastern United States.

2.2.2 2-3 August 1995

A summertime case was selected to coincide with the landfall of hurricane Erin in Florida. Data were collected for the period 09 UTC 02 August 1995 - 03 UTC 03 August 1995. While most of the East Coast was dominated by high pressure and weak flow at all levels, hurricane Erin made landfall in central Florida (near Vero Beach) at 0545 UTC 2 August. While over the Carribean waters, this hurricane had maximum sustained winds of 85 mph, and a central pressure as low as 980 hPa. After landfall, winds dropped to below 70 mph and it was downgraded to Tropical Storm status. At 12 UTC, it was roughly centered over the Florida peninsula, and by 20 UTC its center had moved over the Gulf waters. It subsequently reintensified to hurricane strength and made landfall in the Florida panhandle (in Pensacola Beach) at 1530 UTC 3 August. A secondary feature of interest on this day are the remnants of tropical storm Dean, which were located over parts of Texas, Oklahoma, and Kansas, and which had caused widespread convective rain and flooding.

3 Climatology Database

Climatological fields of mean quantities and their standard deviations are needed within TAP to serve as a background field for the analysis in the case that a short-term forecast is not available. There are several different possible datasets that could be used for defining the mean and standard deviation fields. One set of statistics is available from the National Climatic Data Center (NCDC). They are individual monthly means and selected second moments (variances and cross-products) of winds, height, temperature, and moisture at 9 levels between 1000 hPa and 50 hPa. The statistics were derived from the operational analyses of the National Meteorological Center (NMC). These Climate Diagnostics Data Base (CDDB) datasets are available from the present back to 1978 (1992 for specific humidity and temperature). Long-term climatologies have been computed from the CDDB monthly means for parts of the record: a 10-year climatology is available from the National Center for Atmospheric Research (NCAR), but only for the means of winds, temperature, and geopotential height. A 7-year climatology is also available, which includes the means and second moments of winds, temperature, height, and specific humidity. Because TAP requires statistics for relative humidity, none of these datasets fulfills our requirements. An alternative, readily available dataset was therefore used: a set of monthly means and variances going back over 30 years, based on objectively analyzed radiosonde data. This dataset has been maintained by the Geophysical Fluid Dynamics Laboratory (GFDL) and is described in detail in Oort (1983 [Oor83]). As described in more detail in the next section, it contains information on relative and specific humidity, and has high resolution in the boundary layer (4 levels between 1000 hPa and 850 hPa). Because the analyses do not make use of any first guess or background information, they are most trustworthy over the well-sampled continents, whereas they are based on few data points over large oceanic regions.

3.1 The Oort Radiosonde-Based Dataset

The dataset is described in detail in Oort (1983). The input data used in our processing have the following characteristics:

- Available statistics: Individual monthly means and variances for 1958-1994
- Quantities: u, v (zonal and meridional wind), T (temperature), z (height), q (specific humidity), and RH (relative humidity)
- Grid: 2.5° (latitude) × 5° (longitude)
- Levels (hPa): 1000, 950, 900, 850, 700, 500, 400, 300, 200, 100, 50 (q, RH only to 300 hPa)

3.2 Oort Dataset Processing

3.2.1 Computation of Long-Term Means and Variances

A multi-year climatology was computed from the monthly means in the Oort climatology. All the variables listed above were processed, at all available levels. For each of the 12 months, the long-term mean of the monthly means, the long-term mean of the monthly variances, and the long-term variance of the monthly means were computed for each variable. When used as a background for an analysis, the expected error standard deviation of the mean field is computed as the square root of the sum of the long-term mean of the monthly variance and the long-term variance of the monthly mean.

Most quantities were computed from a 31 year record (January 1959 - December 1989). Because input data were available for shorter periods, the climatology for all points south of 15° S was computed from January 1964 - December 1989 (26 years), and the climatology of RH from January 1974 - December 1989 (16 years).

Before averaging, known deficiencies of the data were removed. In particular, bad values of v at 1000 hPa for May 1978 at 75° longitude were replaced by interpolation between 70° and 80° longitude before averaging; negative values of positive definite quantities (variances of all fields, means of RH and q) were zeroed before averaging; and values at 180° E and 180° W were averaged.

3.2.2 Horizontal Smoothing and Quality Control

Visual examination of the computed climatology revealed that further quality control was needed. In particular, there were some instances of large isolated maxima or minima in the fields (both the mean and interannual variance fields, indicating the presence of one or a few bad individual monthly means in the original data set). Excessively large interannual variances were also found near the poles for some of the variables.

The solution to both problems was to smooth all fields using a nonlinear running filter in the latitude and longitude directions (using the Splus smooth function). Following the smoothing, nonnegative definite quantities (q, RH, and all variances) were reset to be ≥ 0 , and RH and the variance of RH were reset to be ≤ 100 and ≤ 10000, respectively. Before smoothing, the interannual variance was limited to no more than the smoothed long-term mean of the monthly variance.

3.3 Sample Fields and Comparison with CDDB Climatology

Selected fields and levels of the smoothed Oort climatology are shown in Figure 1 for January. For geopotential height, specific humidity, and temperature, shaded plots of the mean are shown with overlaid contours of the standard deviation. In the case of the winds, vector plots of the mean wind field are shown with standard deviations of the vector wind error (computed from the sum of the variances of the wind components). All four plots are shown for 1000 hPa, 500 hPa, and 300 hPa. Only the height and winds are shown for 50 hPa.

Figure 1: Oort climatology maps for January. Mean and standard deviations of geopotential (panels a, e, i, m), vector winds (panels b, f, j, n), specific humidity (panels c, g, k), and temperature (panels d, h, l) at 1000 hPa (panels a-d), 500 hPa (panels e-h), 300 hPa (panels i-l), and 50 hPa (panels m-n). This figure contained in 7 pages is attached.

As is to be expected, the mean fields have a generally smooth appearance, but they clearly contain the salient features of the general circulation: the major baroclinic zone in the tropospheric midlatitudes is evident in the height and temperature maps, and coincides with the belt of strong westerlies. The major regions of cyclogenesis along the east coasts of North America and Asia are associated with a trough in the mean fields. Maxima in the standard deviations are located downwind from the troughs, along the major storm tracks.

The corresponding set of figures for July are shown in Figure 2. They show the typical shift of the strongest baroclinic activity to the Southern Hemisphere. The maps of specific humidity clearly show the effects of the Indian monsoon, in the form of a pronounced maximum of the mean and standard deviation over the area.

Figure 2: Oort climatology maps for July. See Figure 1 for a description of plotted quantities and numbering of panels.

The gross features of the mean atmospheric state as defined by the Oort climatology can also be seen in the meridional cross sections of zonal mean temperature and zonal wind shown in Figure 3. The meridional gradient of temperature, the location and strength of the jet stream, and their variation with the seasons all follow the expected pattern.

Figure 3: Oort climatology meridional cross sections. Zonal mean temperature (shaded) and zonal wind (contours) for January (a) and July (b). This figure is attached.

For purposes of comparison and validation of the climatology dataset computed here, we present horizontal maps for July for the 7-year CDDB climatology dataset obtained from NCAR in Figure 4. Because moisture and temperature data are not available above 500 hPa in this dataset, these fields are not shown at 300 hPa. Comparison with Figure 2 shows similarities in all the major circulation features. The effects of the smoothing of the Oort climatology are evident by the somewhat noisier appearance of the mean and particularly the standard deviation fields in the CDDB data. The meridional cross sections shown in Figure 5 exhibit even fewer differences from the corresponding Oort climatology plots.

Figure 4: CDDB climatology maps for July. Mean and standard deviations of geopotential (panels a, e, i, k), vector winds (panels b, f, j, l), specific humidity (panels c, g), and temperature (panels d, h) at 1000 hPa (panels a-d), 500 hPa (panels e-h), 300 hPa (panels i-j), and 50 hPa (panels k-l). This figure contained in 6-pages is attached.

Figure 5: CDDB climatology meridional cross sections. Zonal mean temperature (shaded) and zonal wind (contours) for January (a) and July (b). This figure is attached.

In summary, then, both a subjective evaluation and comparison with an independent climatology dataset confirm that the Oort climatology dataset derived here provides reasonable values of the required quantities.

4 Error Statistics

Inherent in the modular and extensible design of TAP is the separation of the OI algorithm from the underlying observation and error statistics. The latter are specified through tables that can be tailored to the specific needs if the TAP application. An important part of the TAP project is the development of a statistical data base from which appropriate tables can be selected for different backgrounds, geographic areas, and observing systems.

Correlations of both forecast and observational errors are assumed to be separable and horizontally homogeneous. The error covariances are decomposed in the standard OI fashion:

$$C_{xy} = S_x S_y M_{xy} N_{xy}$$

where x and y are observed or forecast variables at observation or analysis locations; C_{xy} is the covariance between the errors of x and y; S_x is the standard deviation associated with x; S_y is the standard deviation associated with y; M_{xy} is the horizontal correlation between the errors of x and y; and N_{xy} is the vertical correlation between the errors of x and y. In practice, for global analyses the horizontal and vertical correlations may be allowed to vary slowly with vertical and horizontal location. In TAP, they vary geographically as well, but are fixed for a particular case, as decribed here: the horizontal correlations M_{xy} depend on distance and mean pressure and vertical correlations N_{xy} depend on the two pressures. To be precise, M_{xy} is represented by a set of 1–way tables in terms of horizontal distance, for different mean pressure levels, and N_{xy} is a set of 2–way tables in terms of the two pressures. In any particular case, these tables are interpolated as needed. The tables themselves are external to the analysis procedures. Observations of different type are assumed uncorrelated. Different tables are specified for each different observation and background type. For any analysis domain, appropriate versions of M_{xy} and N_{xy} are used. For some backgrounds and observation types, TAP includes different versions of the correlation tables, appropriate for the tropics and extratropics or for the continental and maritime situations. A single one of these is chosen when the analysis segment starts. Estimated prediction error standard deviations are also assumed to be constant in the horizontal in the OI development, but are often specified as a function of position. In TAP, background error standard deviations are either obtained as a gridded field (in the case of a climatology background), or specified for different geographical regions. In the latter case, a single set of standard deviations is chosen for the analysis domain.

To be truly optimal, OI requires perfect statistics. However, estimating the error statistics for the OI analysis requires some compromises. For this reason OI is never truly optimal and is often called statistical interpolation. The basic approach to estimating the required statistics is to collocate everything with radiosondes, collect statistics over time, make many (reasonable) assumptions and deduce various relationships between the statistics (Lorenc 1981; Thiébaux and Pedder 1987 [Lor81, ThiP87]).

The radiosonde errors are considered known. While there have been some explicit studies of the accuracy of radiosondes, it is noted that for the purpose of analysis, scales of variability smaller than the scale of the analysis are usually considered to be noise. Long time periods are desirable to get decent sample sizes for meteorological observations, because temporal correlations reduce the effective sample size considerably. The data are optionally stratified by season to assure stationarity. Collection of data over several years for a given season is desirable.

Unfortunately, for the case of forecast model statistics, models do not stay fixed for long lengths of time. However, modest samples are adequate, considering the simplifications and assumptions made in modeling the statistics. The correlation models employed are quite simple, and the forecast error standard deviations are generally modeled by simple evolution models using empirically determined growth rates and initial conditions from the estimated analysis errors.

The analysis and forecast error magnitudes and their variations with location, season and length of forecast have been studied by many operational centers and researchers (e.g., Lorenz 1982 [Lor82]). The correlation structure of short term (generally 6 hour) forecast errors have also been documented by many centers (Mitchell *et al.*, 1990; Bartello and Mitchell, 1992; Thiébaux *et al.* 1990 [MitCC+90, BarM92, ThiMW90]). At longer ranges much of the research on forecast errors has centered on evaluating model biases, but the operational archives contain large amounts of data, upon which a retrospective study of the forecast error correlations at longer terms (12 to 48 hours) might be based.

During the first year of the TAP project, we have conducted an extensive literature survey and assembled a set of appropriate references for the statistics of forecast model errors, observation errors, and deviations from climatology. An inventory of all references used in our literature survey was constructed, containing a description of the type of statistical information available from each reference. In the following section, information from this inventory is organized by the type of statistics, with a brief description of the most relevant references for each type of statistic. Following this overview of error statistics references, the statistics selected for the baseline version of TAP are described in more detail.

4.1 Overview of Relevant Error Statistics References

4.1.1 Forecast Model Errors

4.1.1.1 Standard Deviations

[BarM92]: Figure of Canadian Meteorological Centre operational model errors of heights and winds as a function of pressure.

[Ben89]: tables of background error standard deviations of height, temperature, relative humidity, and wind used in the MAPS (now called the Rapid Update Cycle, or RUC) isentropic analysis system. The background is NMC's 12-hour NGM forecast.

[BenSM+91, Car91, DevS94]: provide updated values for the statistics in [Ben89] for 3-hour forecasts from the RUC forecast model, for Montgomery potential, pressure, winds, and humidity (condensation pressure).

[Ber79, McPBK+79]: NMC global prediction model errors for temperature, winds, and specific humidity at mandatory pressure levels. Prediction error growth rates for NMC global model.

[DeyM85]: NMC global spectral model 6-hour forecast errors for temperature and winds at 12 mandatory pressure levels, for the extratropics and tropics.

[HolL86, LonH86]: ECMWF global grid point model 6-hour forecast errors for winds, height, and virtual temperature.

[Lor81, LonSU92]: ECMWF forecast errors used in the ECMWF OI for heights, winds, humidity, and thickness, separately for extratropics and tropics.

[GoeP93]: NOGAPS global 6-hour forecast errors used in the Navy OI for height, wind, and thickness.

4.1.1.2 Horizontal Correlations

[Ben89]: Second-order autocorrelation function fits of correlation on isentropic surfaces for NMC's 12-hour NGM forecast.

[Car91, SchC91, DevS94]: provide updated values for the correlations on isentropic surfaces for 3-hour forecasts from the RUC forecast model, for Montgomery potential, pressure, winds, and humidity (condensation pressure).

[DeyM85]: Functional fits for height and humidity error correlations.

[BarM92]: Figure of Canadian Meteorological Centre operational forecast model error correlations for 250 mb winds and 700 mb heights. Sample 2-d and 3-d correlation plots for heights, winds, height-winds.

[HolL86, LonH86]: ECMWF global grid point model 6-hour forecast error correlations for longitudinal and transverse winds, height, and wind-height cross-correlations.

[Lor81, LonSU92]: ECMWF forecast error correlations used in the ECMWF OI for heights, longitudinal and transverse winds, height-wind cross-correlations, humidity, and thickness, separately for extratropics and tropics.

[GoeP93]: NOGAPS global 6-hour forecast error correlations for heights, transverse and longitudinal winds, and height-wind cross-correlations.

4.1.1.3 Vertical Correlations

[Ben89]: Vertical correlation matrix for u-component of wind for NMC's 12–hour NGM forecast.

[DeyM85]: Functional fits for height error correlations.

[BarM92]: Canadian Meteorological Centre operational forecast model vertical error correlations for height, wind, and height–wind correlations.

[HolL86, LonH86]: ECMWF global grid point model 6-hour forecast errors vertical correlations for longitudinal and transverse winds, and height.

[LonSU92]: ECMWF forecast error correlations used in the ECMWF OI for heights and longitudinal and transverse winds.

[GoeP93]: NOGAPS global 6-hour forecast error vertical correlations for heights and transverse and longitudinal winds.

4.1.2 Climatology Background Errors

4.1.2.1 Standard Deviations Background error standard deviations for the climatology background are obtained from the climatological variance itself, which is available in gridded form (see Section 3).

4.1.2.2 Horizontal Correlations

[Bue71, Bue72]: Plots and functional fits of 500 mb and 200 mb wind and height correlation for summer and winter over Northern Hemisphere continents.

[JulT75, Thi75, Thi76, Thi77, Thi85]: 500 mb height, temperature, and wind correlations and functional fits.

[RamKS73]: 500 mb wind correlations over Indian region.

4.1.2.3 Vertical Correlations No references have been found with tables or functional fits for vertical correlations of climatology background errors. However, numerous datasets exist from which this information has already been and easily can be computed.

4.1.3 Observation Errors

4.1.3.1 Standard Deviations

[Ben89]: OESDs for height, temperature, relative humidity, and wind for rawinsonde, profiler, aircraft, and surface observations.

[Car91]: rawinsonde OESDs for Montgomery potential, pressure, winds, and humidity (condensation pressure) at several isentropic levels.

[Ber79]: Temperature and wind errors for rawinsonde, aircraft, satellite retrievals, and cloud drift winds.

[DeyM85]: Temperature and wind errors for rawinsonde, aircraft, satellite retrievals, and cloud drift winds.

[LonSU92]: Temperature, height, thickness, wind, and humidity errors for rawinsonde, aircraft, satellite retrievals, and cloud drift winds, surface observations, drifting buoys, and pilot balloons.

[Lor81]: Temperature, height, thickness, and wind errors for rawinsonde and aircraft observations.

[GoeP93]: Temperature, height, thickness, and wind errors for rawinsonde, aircraft, satellite retrievals, cloud drift winds, and surface observations.

4.1.3.2 Horizontal Correlations

[DeyM85]: horizontal correlations of satellite retrieved thickness errors.

[LonSU92]: horizontal correlations of satellite retrieved thickness errors.

4.1.3.3 Vertical Correlations

[Ber79]: Rawinsonde error vertical correlations for winds and geopotential. Satellite height error correlations.

[HolL86, LonH86]: Rawinsonde error vertical correlations for winds, geopotential, and thickness.

[LonSU92]: Rawinsonde error vertical correlations for geopotential, satellite retrieval thickness error vertical correlation.

[GoeP93]: Radiosonde height error vertical correlation.

4.2 Tap Baseline Error Statistics References

The error statistics for the baseline version of TAP rely most heavily on the statistics used in NOGAPS (Goerss and Phoebus, 1993 [GoeP93]). The primary reason is that the most likely scenario for a TAP implementation is for global forecast model background fields obtained from the Navy NOGAPS model. The NOGAPS model error statistics are thus most relevant to TAP. Furthermore, the Navy NOGAPS system is a state of the art operational system with recent and fairly complete and accessible documentation. These statistics have been supplemented where needed with information from other sources from the above list, in most cases from the ECMWF documentation found in Lönnberg *et al.* (1992 [LonSU92]). Elements for which no source has yet been selected have been marked by "TBD". Where no entry for correlations exists, autocorrelations are assumed to be zero except at zero separation, and crosscorrelations are assumed to be zero. At present, a final selection of background error statistics for climatology has not been made.

4.2.1 Forecast Model Errors

4.2.1.1 Standard Deviations These standard deviations have all been derived from comparisons with radiosonde data over well-sampled regions. As a possible enhancement, these values could be inflated by an appropriate error growth rate over data-sparse regions.

height: [GoeP93, Tables on p. 41]

temperature: TBD

thickness: computed from height error covariances

winds: [GoeP93, Tables on p. 41]

relative humidity: [LonSU92, p.3.5]

4.2.1.2 Horizontal Correlations

height: [GoeP93, eq. 30, p.12-13]

thickness: computed from height error covariances

winds: [GoeP93, eq. 31-41, p.13-14]

height–winds crosscorrelations: [GoeP93, eq. 31-41, p.13-14]

relative humidity: [LonSU92, p. 3.5]

4.2.1.3 Vertical Correlations

height: [GoeP93, p.18]

thickness: computed from height error covariances

winds: [GoeP93, p.18]

4.2.2 Observation Errors

The observation errors in these references have not been adjusted for the representational error (*i.e.*, the representational error has not been separated from the instrument error). This is left as an enhancement to the statistical database.

4.2.2.1 Standard Deviations

rawinsonde: height: [GoeP93, Tables on p.41]

temperature: TBD

thickness: computed from height error covariances

winds: [GoeP93, Tables on p.41]

relative humidity: [LonSU92, p.3.1]

aircraft winds: [GoeP93, Tables on p.41]

satellite retrievals: thickness: [GoeP93, Tables on p.41]

temperature: [LonSU92, p.2.36]

relative humidity: [LonSU92, p.3.4]

cloud drift winds: [GoeP93, Tables on p.41]

surface observations: height: [LonSU92, p. 2.35]

relative humidity: [LonSU92, p.3.1-3.3]

4.2.2.2 Horizontal Correlations

satellite thickness: [LonSU92, p. 2.37]

cloud drift wind: TBD

4.2.2.3 Vertical Correlations

rawinsonde height: [GoeP93, p. 17]

satellite thickness: [LonSU92, p. 2.39]

5 Prototype System Development

The algorithm prototyping during the first year of the TAP project has resulted in a preliminary end-to-end analysis system, from setup functions (selection of analysis points, background and data sources), preprocessing, analysis, postprocessing, to graphical display. The analysis is limited to a scalar analysis at this point, and some parts of the full system design are either replaced by Splus library functions or omitted until they are coded and unit tested. The system at this stage is capable of ingesting climatological or forecast background fields on a large variety of grids, and conventional upper air data.

End-to-end tests of this prototype have been performed using the real data collected for the 6 March 1995 case. The ETA-model 12-hour forecast of 850 hPa height valid at 12 UTC 6 March 1995 is shown in Figure 6 over a portion of the native ETA model grid. The same field is shown in the bottom panel of the figure after interpolation to a hypothetic analysis grid, which, in this case, is a polar stereographic grid rotated with respect to the

ETA model grid. A comparison of the analysis values produced by the prototype system with the radiosonde observations plotted in Figure 6 demonstrate the success of the analysis procedure: the first guess is modified toward a closer agreement with the observations. The plot of the analysis increments in Figure 6 allows a closer examination of the modification of the background field. The magnitude of the increments are controlled by the choice of the observation and background error standard deviations. For this system test, radiosonde errors were set at approximately half the forecast error magnitude.

Figure 6: Eta-based analysis plots. The 12-hr ETA-model forecast of 850 hPa for 12 UTC 6 March 1995 is shown on a portion of the native model grid (a) and the chosen analysis grid (b). Also shown are a contour plot of the analysis overlaid over a station plot of the radiosonde observations (c), and a contour plot of the analysis increments (d). This figure contained in 4 pages is attached.

A second set of plots is shown in Figure 7 for the case when climatology is used as the background. As in Figure 6, the background field of 850 hPa height over the area is shown on the native grid of the background field (in this case, the lat-lon grid of the climatological data base), and after interpolation to the same analysis grid used in Figure 6. As is to be expected, this background field is more nearly zonal, and completely lacks the low pressure system over Southern Canada. The analysis shown in Figure 7 more closely resembles the ETA-based analysis shown in Figure 6, although the effects of the smooth background are still visible in the form of less intense low centers and larger differences from the observations. The analysis increments shown in Figure 7 are much larger than those in Figure 6, both because the observation increments are larger, and because the analysis drew closer to the observations (observation errors were assumed to be 4-7 times smaller than background errors).

Figure 7: Climatology-based analysis plots. The climatology background of 850 hPa for 12 UTC 6 March 1995 is shown on a portion of the lat-lon grid and the chosen analysis grid. Also shown are a contour plot of the analysis overlaid over a station plot of the radiosonde observations, and a contour plot of the analysis increments. This figure is attached.

References

[BarM92] P. Bartello and H. L. Mitchell. A continuous three-dimensional model of short-range forecast error covariances. *Tellus*, 44A:217–235, 1992.

[Ben89] S. G. Benjamin. An isentropic mesoα-scale analysis system and its sensitivity to aircraft and surface observations. *Monthly Weather Review*, 117:1586–1603, 1989.

[BenSM+91] S. G. Benjamin, T. L. Smith, P. A. Miller, D. Kim, T. W. Schlatter, and R. Bleck. Recent improvements in the maps isentropic-sigma data assimilation system. In *Preprints, Ninth Conference on Numerical Weather Prediction*, pages 118–121, Denver, CO, 1991. Amer. Meteorol. Soc.

[Ber79] K. H. Bergman. Multivariate analysis of temperature and winds using optimum interpolation. *Monthly Weather Review*, 107:1423–1444, 1979.

[Bue71] C. E. Buell. Two-point wind correlations on an isobaric surface in a nonhomogeneous non-isotropic atmosphere. *Journal of Applied Meteorology*, 10:1266–1274, 1971.

[Bue72] C. E. Buell. Correlation functions for wind and geopotential on isobaric surfaces. *Journal of Applied Meteorology*, 11:51–59, 1972.

[Car91] Jean-Marie Carrière. Statistics of horizontal correlation of errors for three-hour prediction fields in isentropic coordinates. In *Preprints, Ninth Conference on Numerical Weather Prediction*, pages 62–65, Denver, Colorado, 14-18 October 1991. American Meteorological Society, Boston, MA.

[DevS94] D. Dèvènyi and T. W. Schlatter. Statistical properties of three-hour prediction "errors" derived from the Mesoscale Analysis and Prediction System. *Mon. Wea. Rev.*, 122(6):1263–1280, 1994.

[DeyM85] C. H. Dey and L. L. Morone. Evolution of the National Meteorological Center global data assimilation system: January 1982-December 1983. *Monthly Weather Review*, 113:304–318, 1985.

[GoeP93] James S. Goerss and Patricia A. Phoebus. The multivariate optimum interpolation analysis of meteorological data at the Fleet Numerical Oceanography Center. FR 7531-92-9413, Navy Research Laboratory, Monterey CA, April 1993.

[HolL86] A. Hollingsworth and P. Lönnberg. The statistical structure of short-range forecast errors as determined from radiosonde data. Part I: The wind field. *Tellus*, 38A:111–136, 1986.

[JulT75] P. R. Julian and H. J. Thiébaux. On some properties of correlation functions used in optimum interpolation schemes. *Monthly Weather Review*, 103:605–616, 1975.

[LonH86] P. Lönnberg and A. Hollingsworth. The statistical structure of short-range forecast errors as determined from the radiosonde data. Part II: The covariance of height and wind errors. *Tellus*, 38A:137–161, 1986.

[LonSU92] P. Lönnberg, D. Shaw, and P Undén, editors. *Research Manual 1, ECMWF Data Assimilation, Scientific Documentation.* ECMWF, Reading, U.K., 1992.

[Lor81] A. Lorenc. A global three-dimensional multivariate statistical interpolation scheme. *Monthly Weather Review*, 109:701–721, 1981.

[Lor82] E. N. Lorenz. Atmospheric predictability experiments with a large numerical model. *Tellus*, 34:505–513, 1982.

[McPBK+79] R. D. McPherson, K. H. Bergman, R. E. Kistler, G. E. Rasch, and D. S. Gordon. The NMC operational global data assimilation system. *Monthly Weather Review*, 107:1445–1461, 1979.

[MitCC+90] Herschel L. Mitchell, Cécilien Charette, Clément Chouinard, and Bruce Brasnett. Revised interpolation statistics for the Canadian data assimilation procedure: Their derivation and application. *Monthly Weather Review*, 118:1591–1614, 1990.

[Oor83] A. H. Oort. Global atmospheric circulation statistics. Professional Paper 14, NOAA, Washington, DC, 1983. [NTIS PB8-4-129717].

[RamKS73] Y. Ramanathan, P. Kulkarni, and D. R. Sikka. On a study of winter season wind structure at 500 mb in the Indian region for use in objective analysis of the wind field. *Journal of Applied Meteorology*, 12, 1973.

[SchC91] Thomas W. Schlatter and Jean-Marie Carrière. A correlation model allowing for divergent wind analyses and supporting three-hour assimilation of mesoscale data. In *Preprints, Ninth Conference on Numerical Weather Prediction*, pages 58–61, Denver, Colorado, 14-18 October 1991. American Meteorological Society, Boston, MA.

[Thi85] H. J. Thiébaux. On approximations to geopotential and wind-field correlation structures. *Tellus*, 37A:126–131, 1985.

[ThiMW90] H. J. Thiébaux, L. L. Morone, and R. L. Wobus. Global forecast error correlation. Part 1: Isobaric wind and geopotential. *Monthly Weather Review*, 118:2117–2137, 1990.

[ThiP87] H. J. Thiébaux and M. A. Pedder. *Spatial Objective Analysis: With Applications in Atmospheric Science.* Academic, London, 1987.

[Thi75] H. Jean Thiébaux. Experiments with correlation representations for objective analysis. *Monthly Weather Review*, 103:617–627, 1975.

[Thi76] H. Jean Thiébaux. Anisotropic correlation functions for objective analysis. *Monthly Weather Review*, 104:994–1002, 1976.

[Thi77] H. Jean Thiébaux. Extending estimation accuracy with anisotropic interpolation. *Monthly Weather Review*, 105:691–699, 1977.

Figure 1

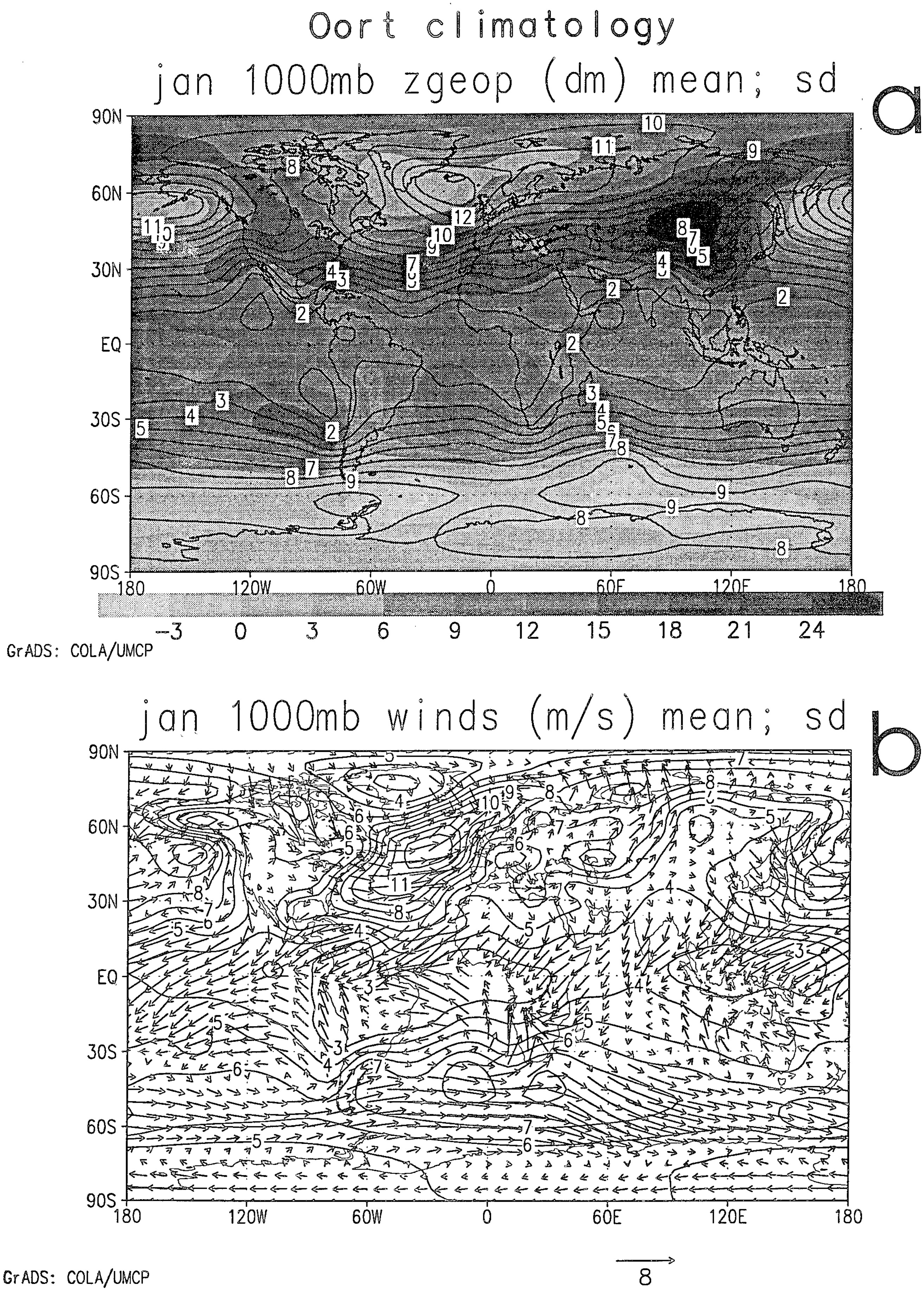

Oort climatology
jan 1000mb zgeop (dm) mean; sd
a
90N
60N
30N
EQ
30S
60S
90S
180
120W
60W
0
60E
120E
180
−3
0
3
6
9
12
15
18
21
24
GrADS: COLA/UMCP
jan 1000mb winds (m/s) mean; sd
b
90N
60N
30N
EQ
30S
60S
90S
180
120W
60W
0
60E
120E
180
8
GrADS: COLA/UMCP

Figure 1

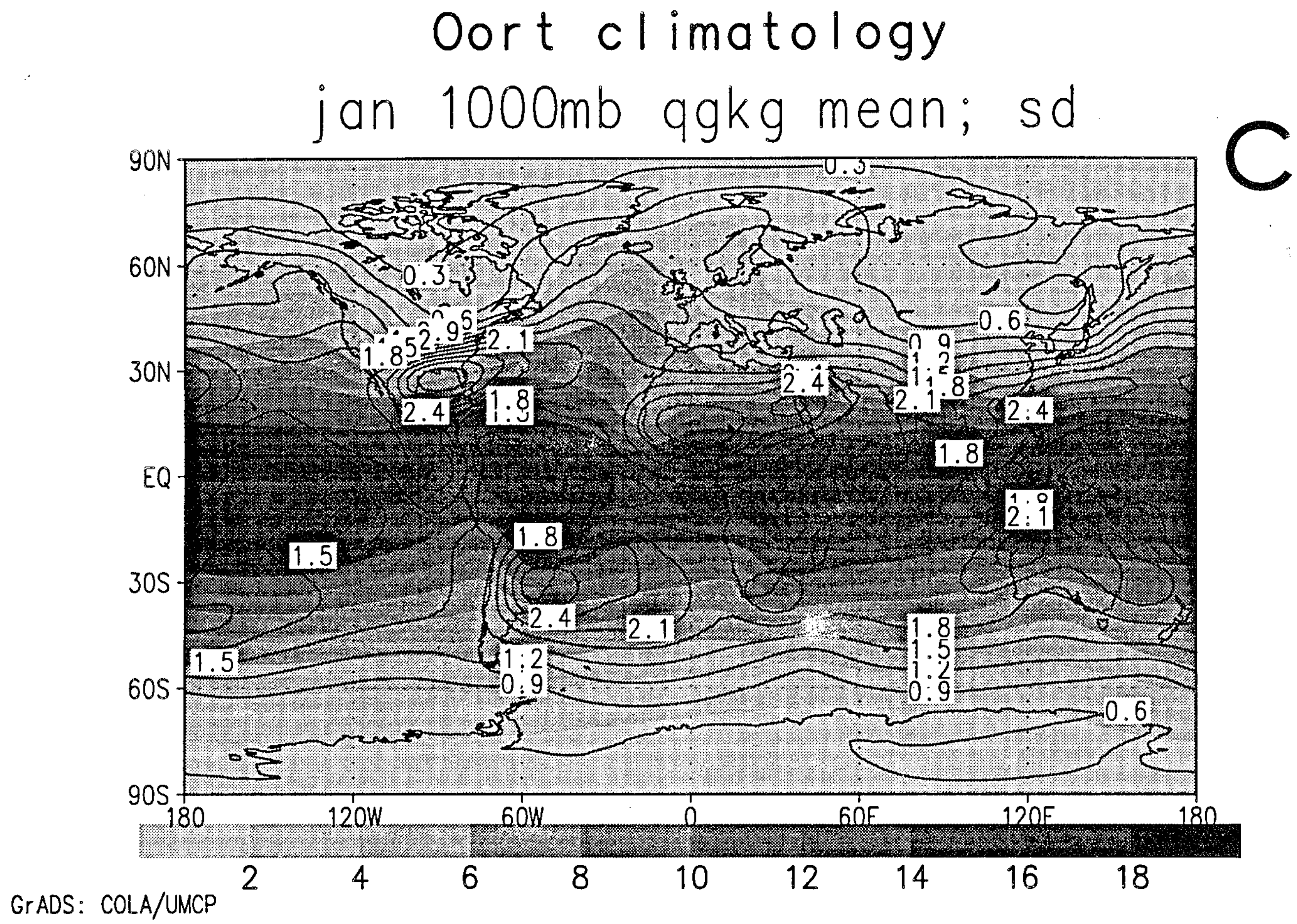
Oort climatology
jan 1000mb qgkg mean; sd
c
90N
60N
30N
EQ
30S
60S
90S
180
120W
60W
0
60E
120E
180
2
4
6
8
10
12
14
16
18
GrADS: COLA/UMCP

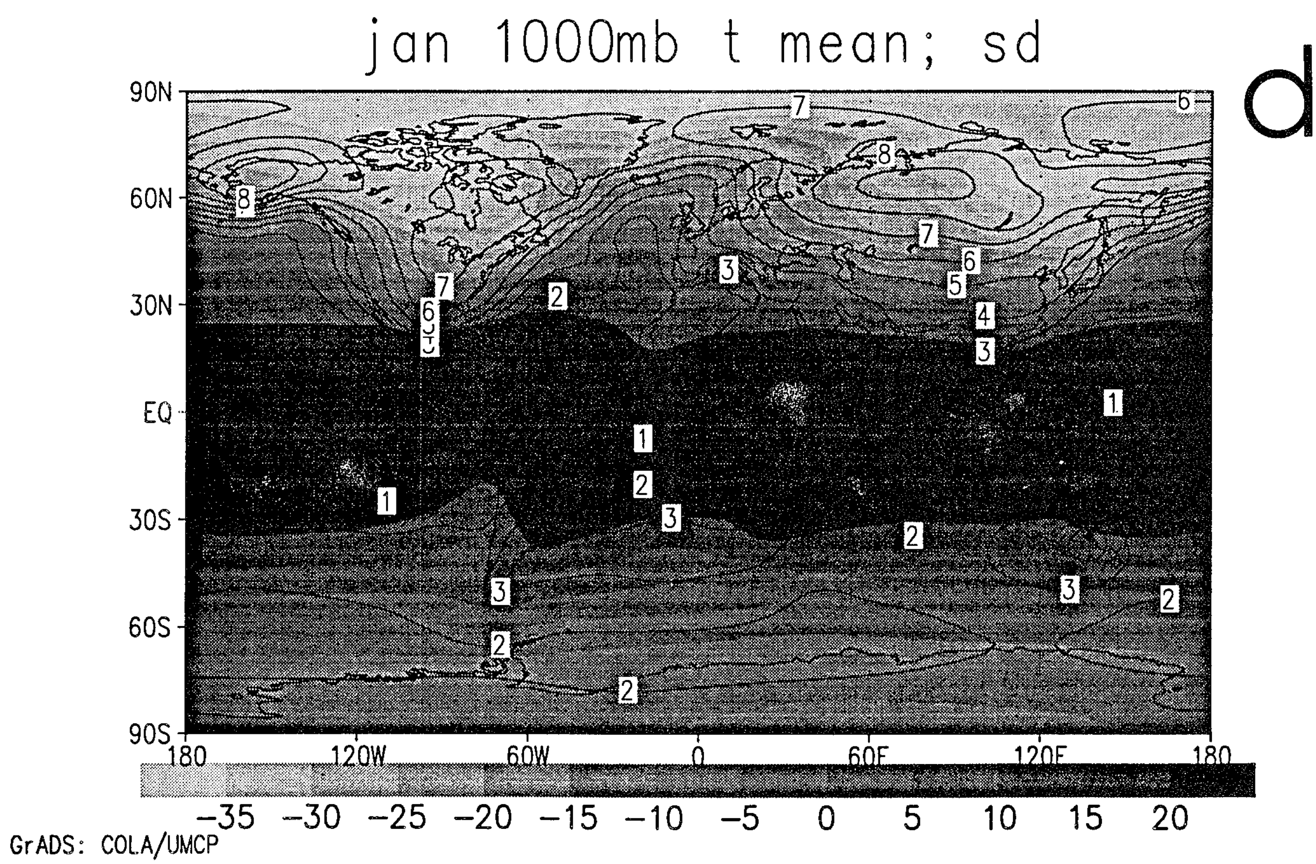
jan 1000mb t mean; sd
d
90N
60N
30N
EQ
30S
60S
90S
180
120W
60W
0
60E
120E
180
−35
−30
−25
−20
−15
−10
−5
0
5
10
15
20
GrADS: COLA/UMCP

Figure 1

Oort climatology

jan 500mb zgeop (dm) mean; sd

e

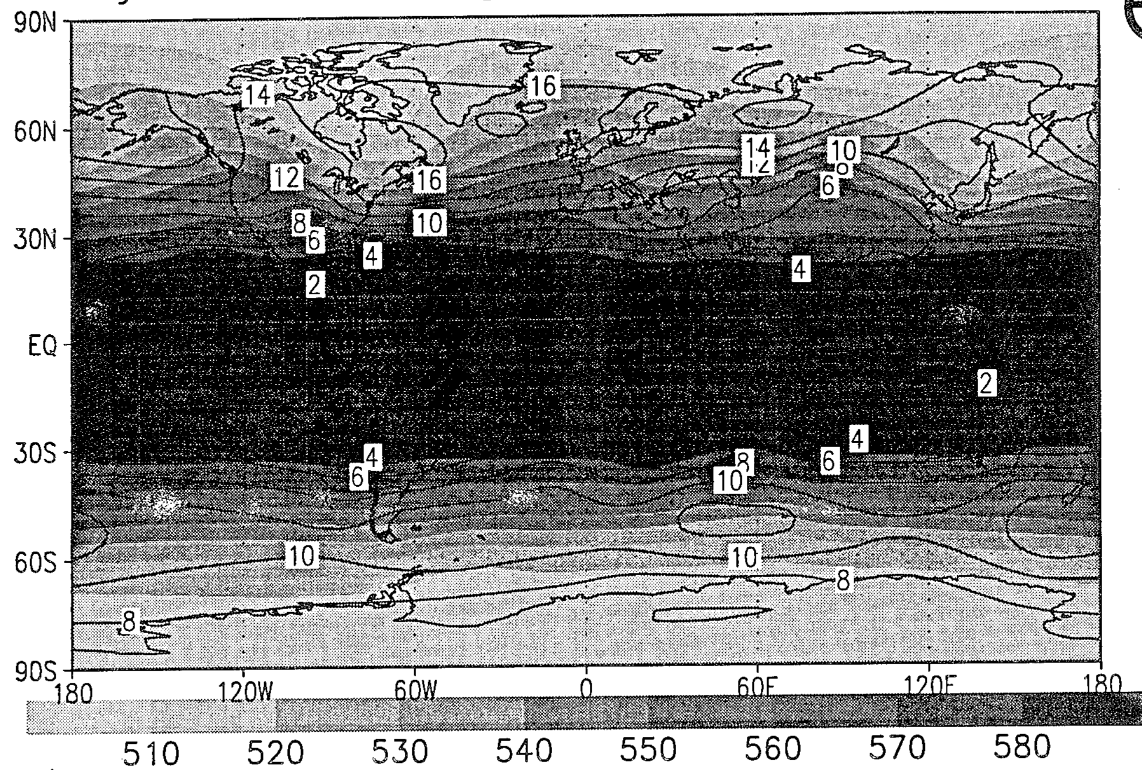

GrADS: COLA/UMCP

jan 500mb winds (m/s) mean; sd

f

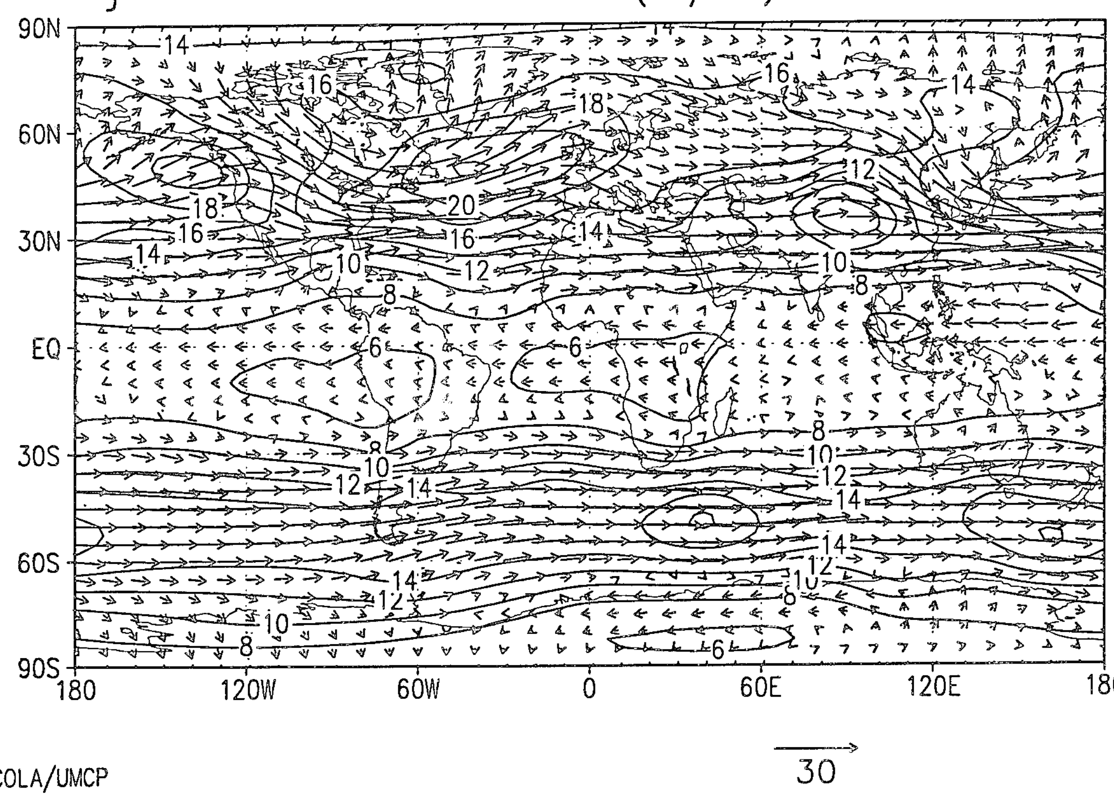

GrADS: COLA/UMCP

Figure 1

Oort climatology

jan 500mb qgkg mean; sd

g

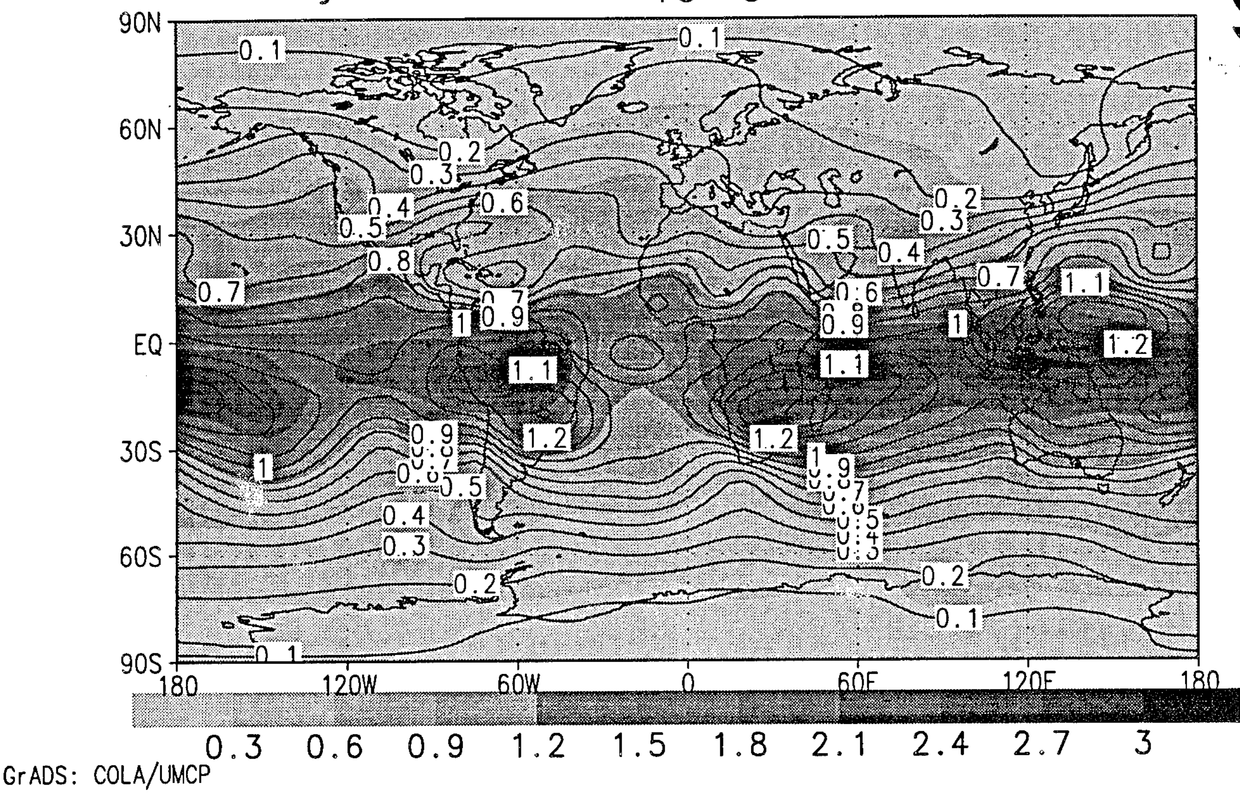

jan 500mb t mean; sd

h

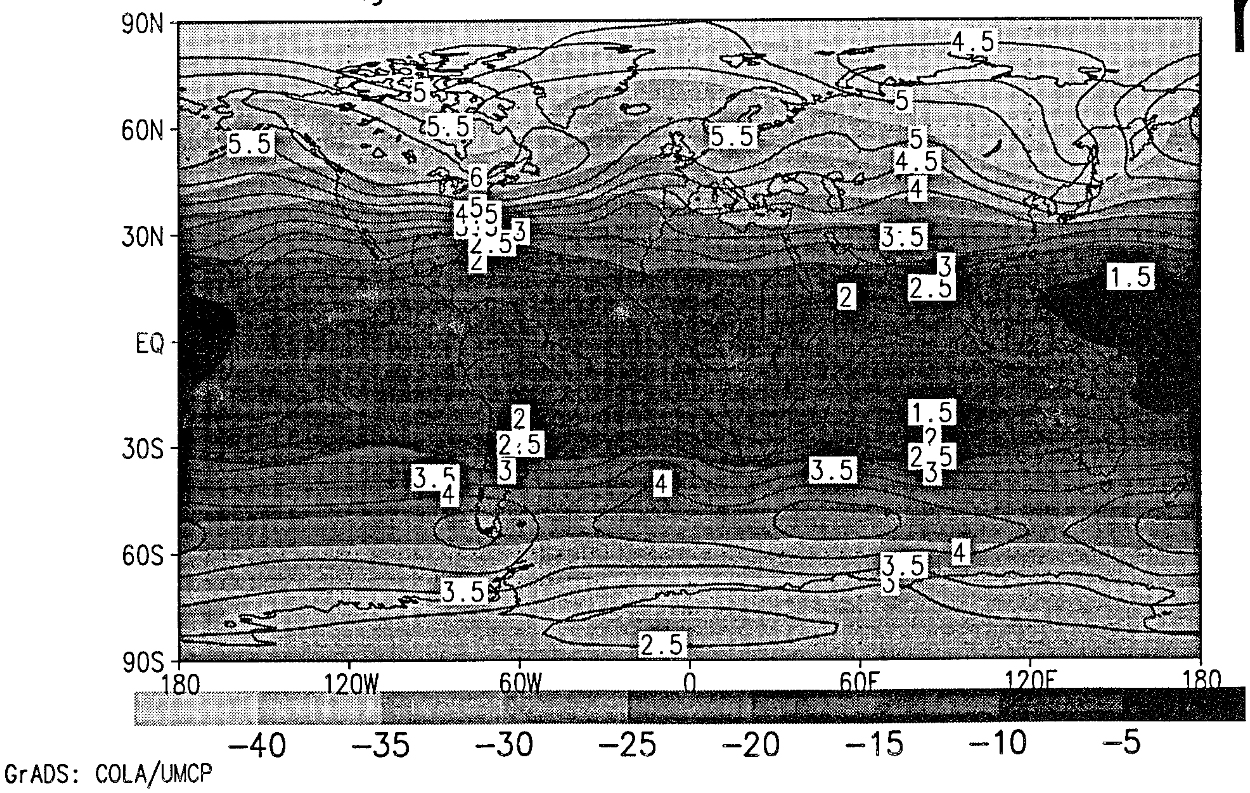

Figure 1

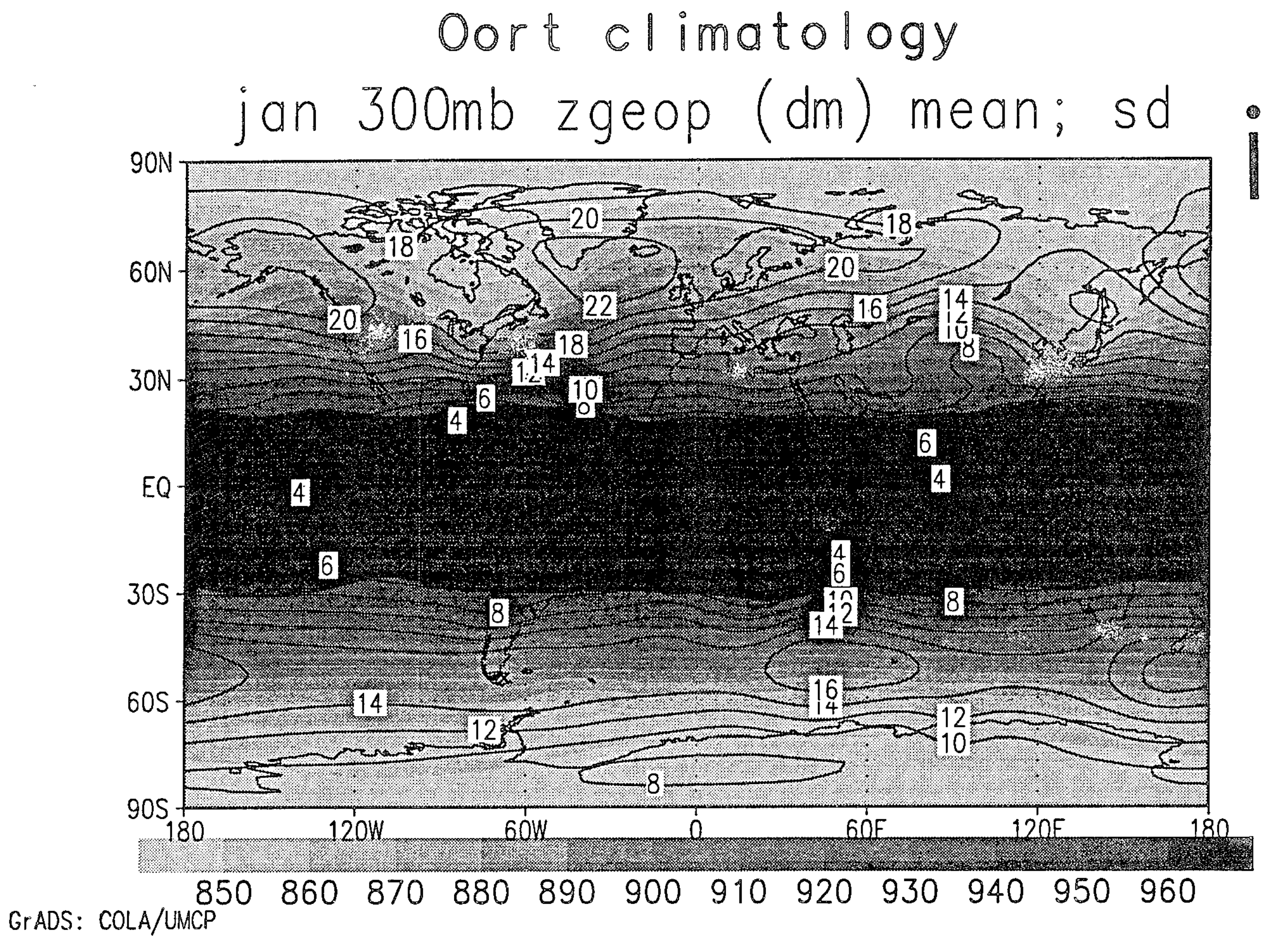
Oort climatology
jan 300mb zgeop (dm) mean; sd
90N
60N
30N
EQ
30S
60S
90S
180
120W
60W
0
60E
120E
180
850 860 870 880 890 900 910 920 930 940 950 960
GrADS: COLA/UMCP

i

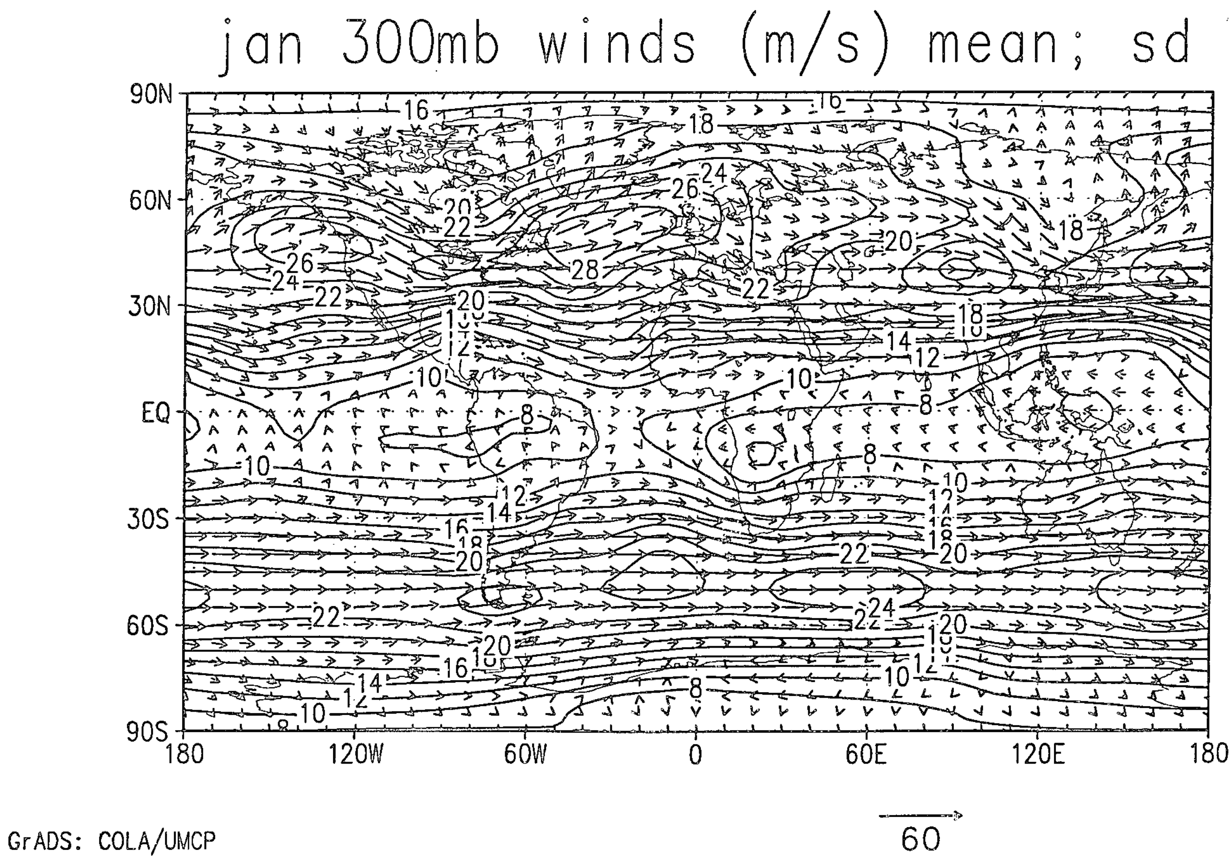
jan 300mb winds (m/s) mean; sd
90N
60N
30N
EQ
30S
60S
90S
180
120W
60W
0
60E
120E
180
60
GrADS: COLA/UMCP

j

Figure 1

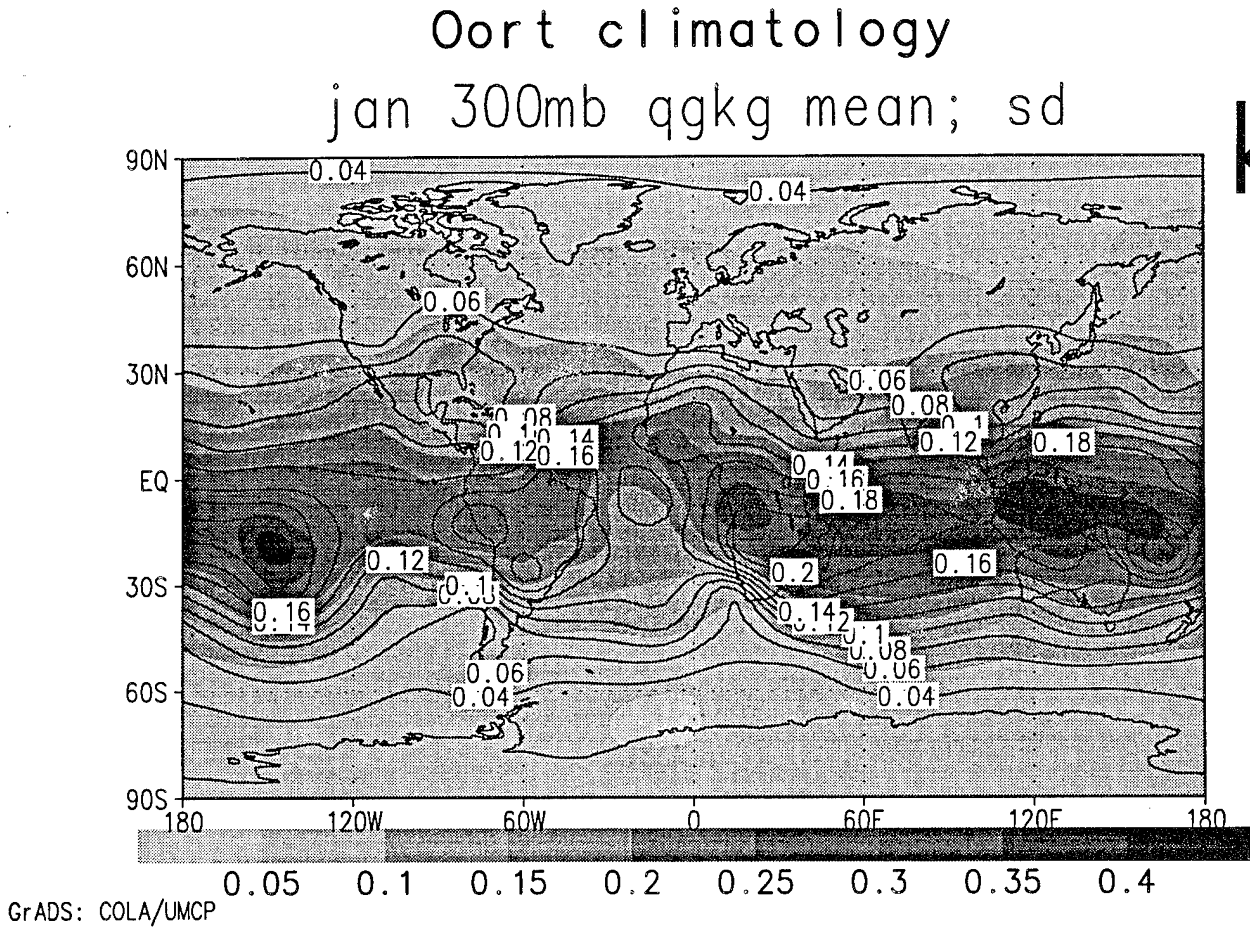
Oort climatology
jan 300mb qgkg mean; sd
90N
60N
30N
EQ
30S
60S
90S
180
120W
60W
0
60E
120E
180
0.05
0.1
0.15
0.2
0.25
0.3
0.35
0.4
GrADS: COLA/UMCP

K

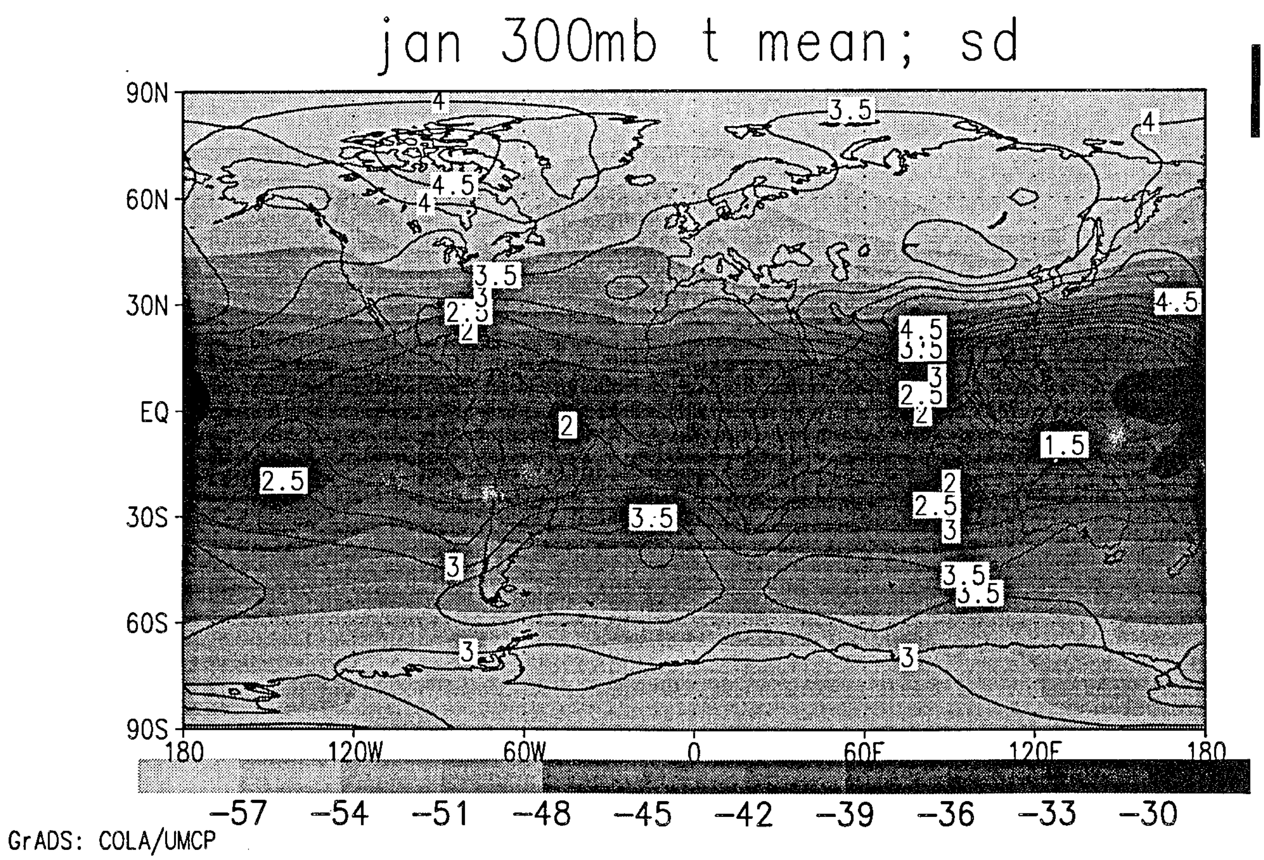
jan 300mb t mean; sd
90N
60N
30N
EQ
30S
60S
90S
180
120W
60W
0
60E
120E
180
−57
−54
−51
−48
−45
−42
−39
−36
−33
−30
GrADS: COLA/UMCP

l

Figure 1

Oort climatology

jan 50mb zgeop (dm) mean; sd

m

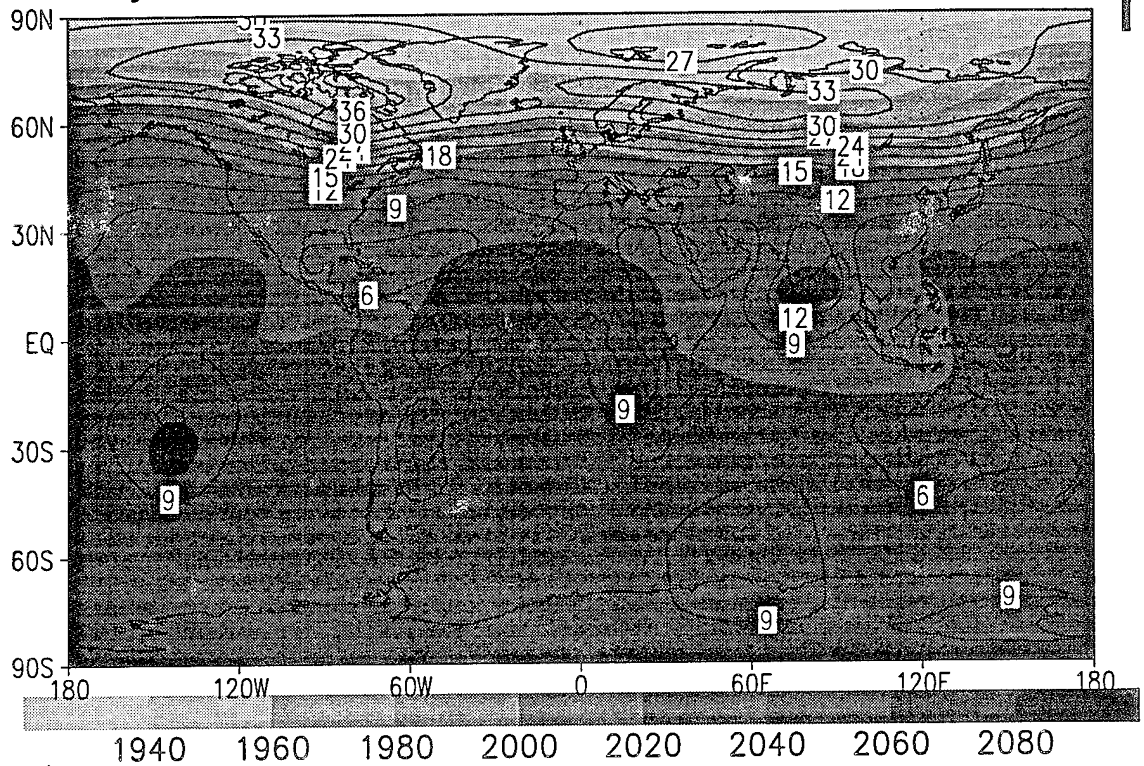

GrADS: COLA/UMCP

jan 50mb winds (m/s) mean; sd

n

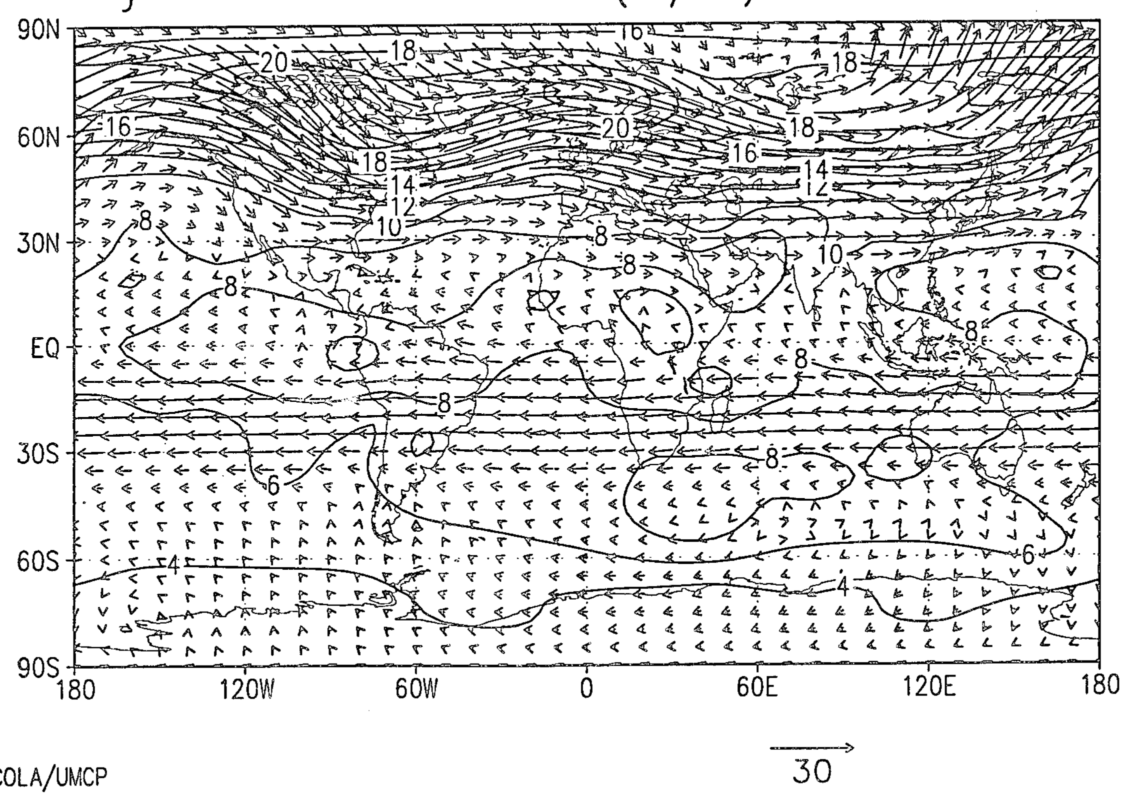

GrADS: COLA/UMCP

Figure 2

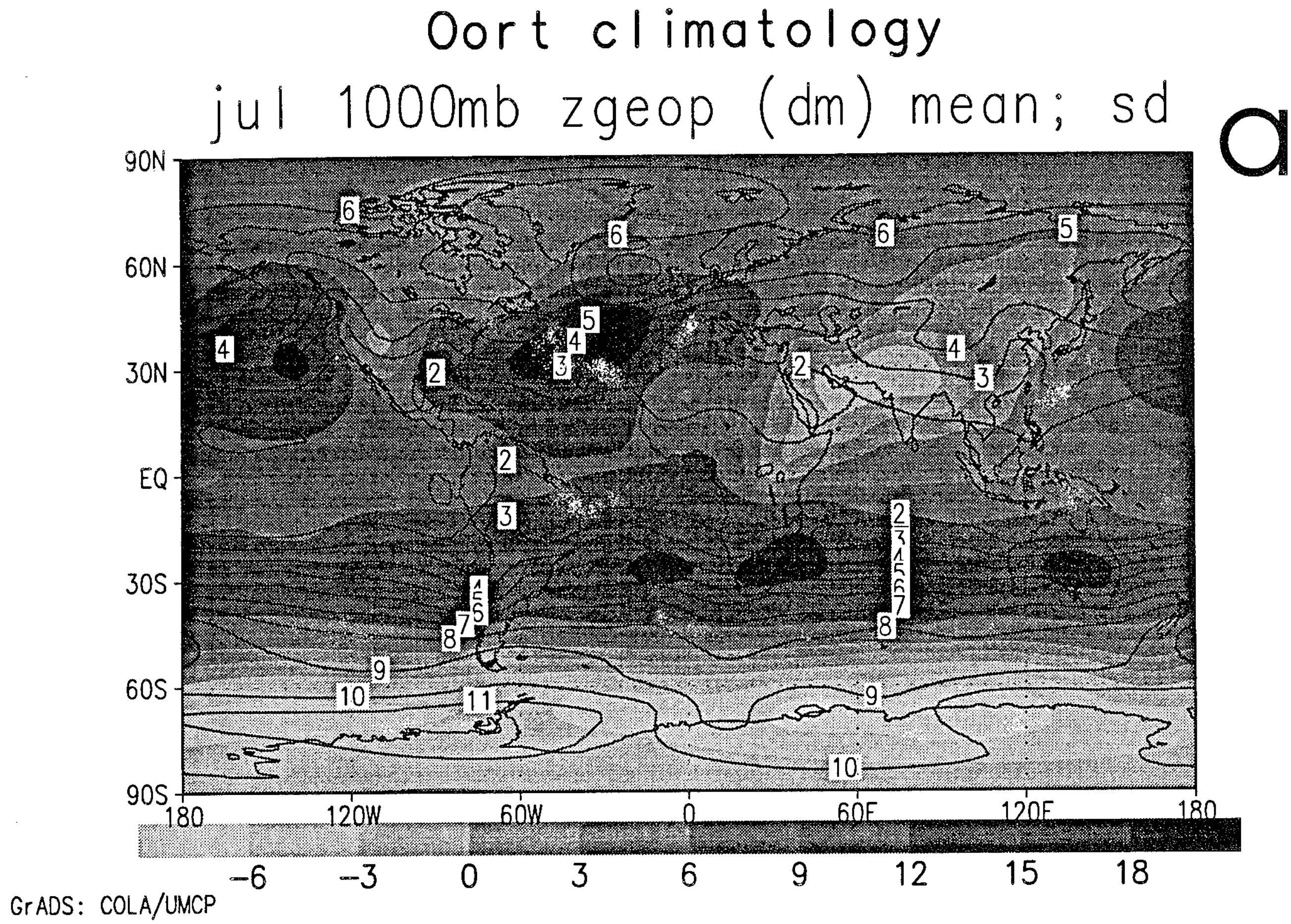

Oort climatology
jul 1000mb zgeop (dm) mean; sd
a
90N
60N
30N
EQ
30S
60S
90S
180
120W
60W
0
60E
120E
180
-6
-3
0
3
6
9
12
15
18
GrADS: COLA/UMCP

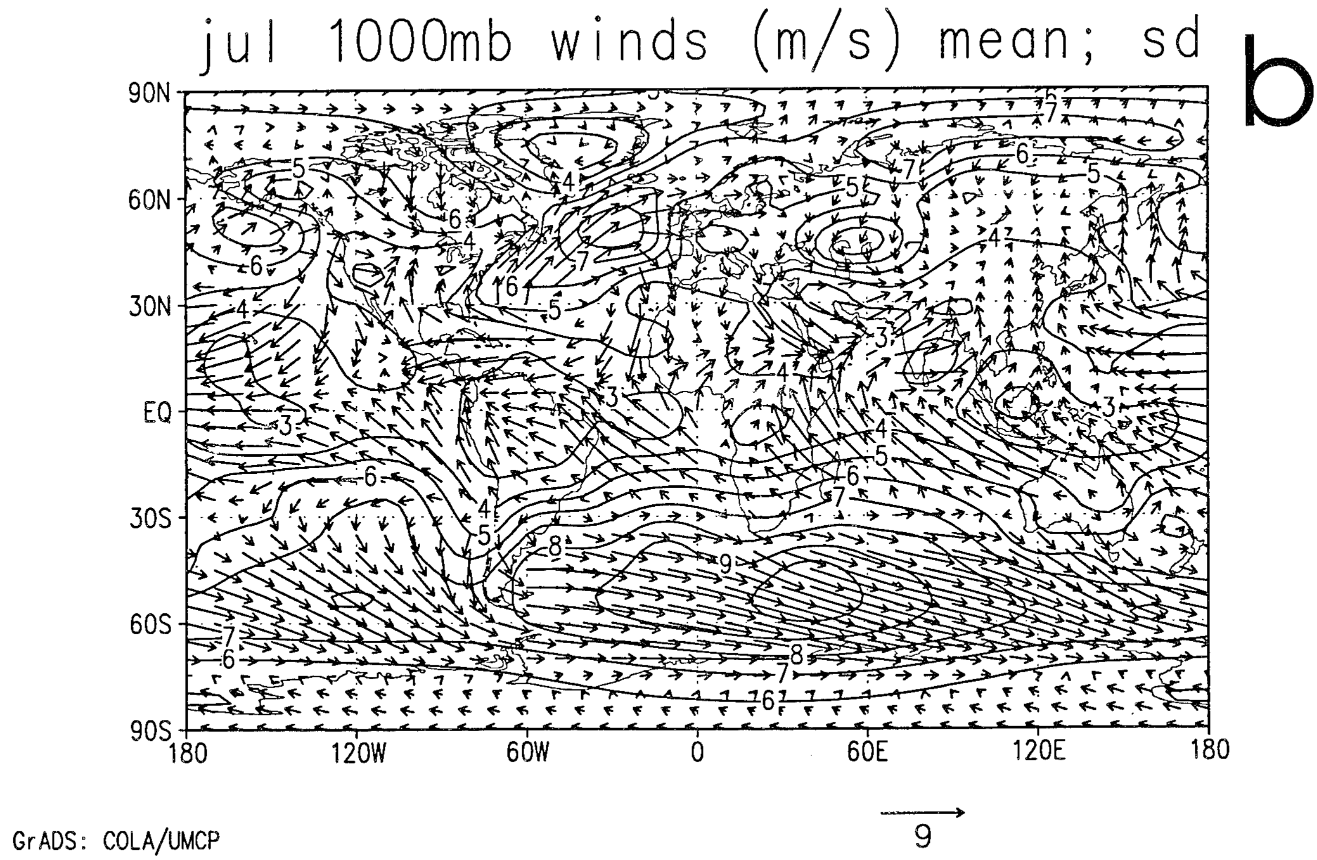

jul 1000mb winds (m/s) mean; sd
b
90N
60N
30N
EQ
30S
60S
90S
180
120W
60W
0
60E
120E
180
9
GrADS: COLA/UMCP

Figure 2

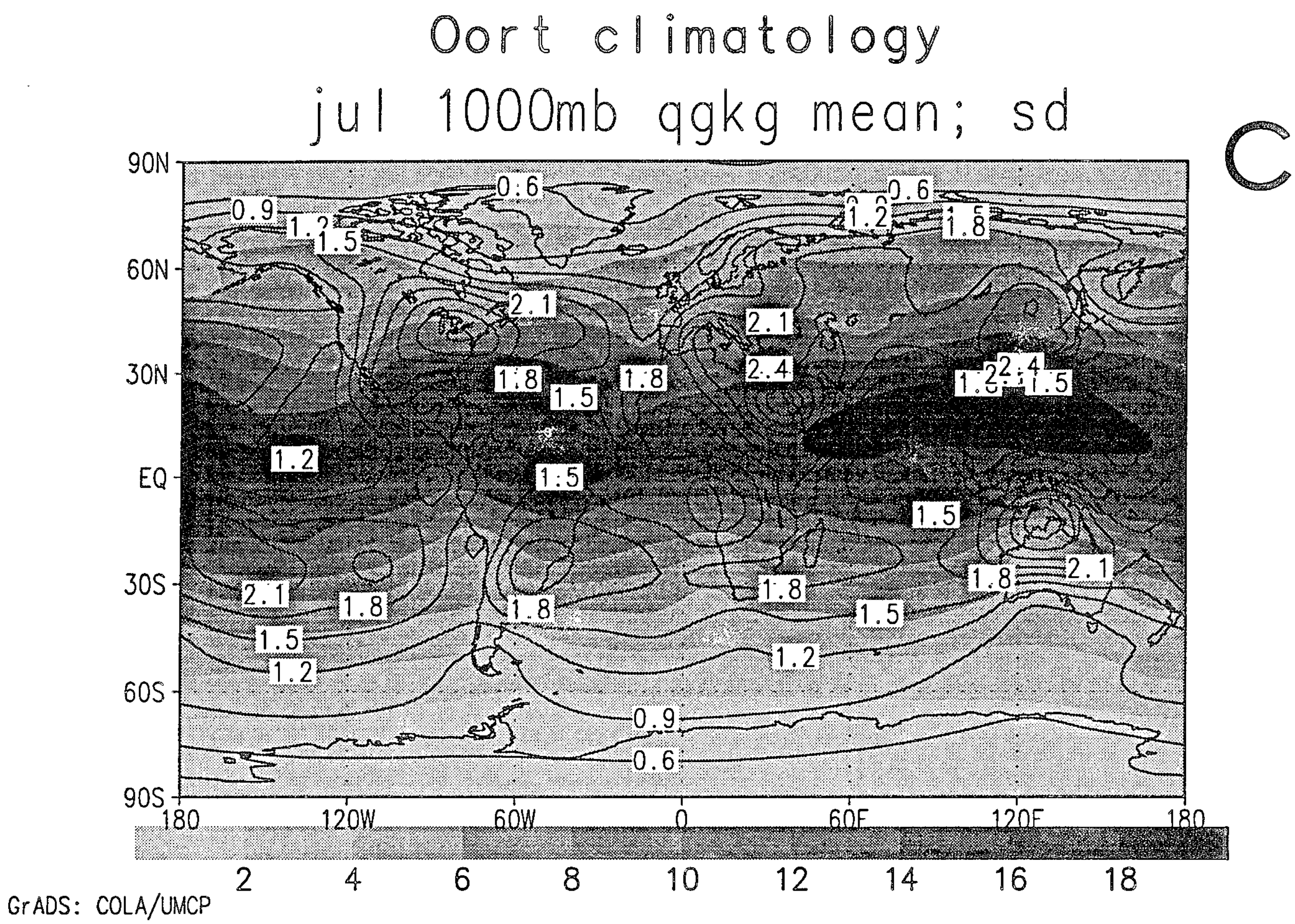

Oort climatology
jul 1000mb qgkg mean; sd
c
90N
60N
30N
EQ
30S
60S
90S
180
120W
60W
0
60E
120E
180
2
4
6
8
10
12
14
16
18
GrADS: COLA/UMCP

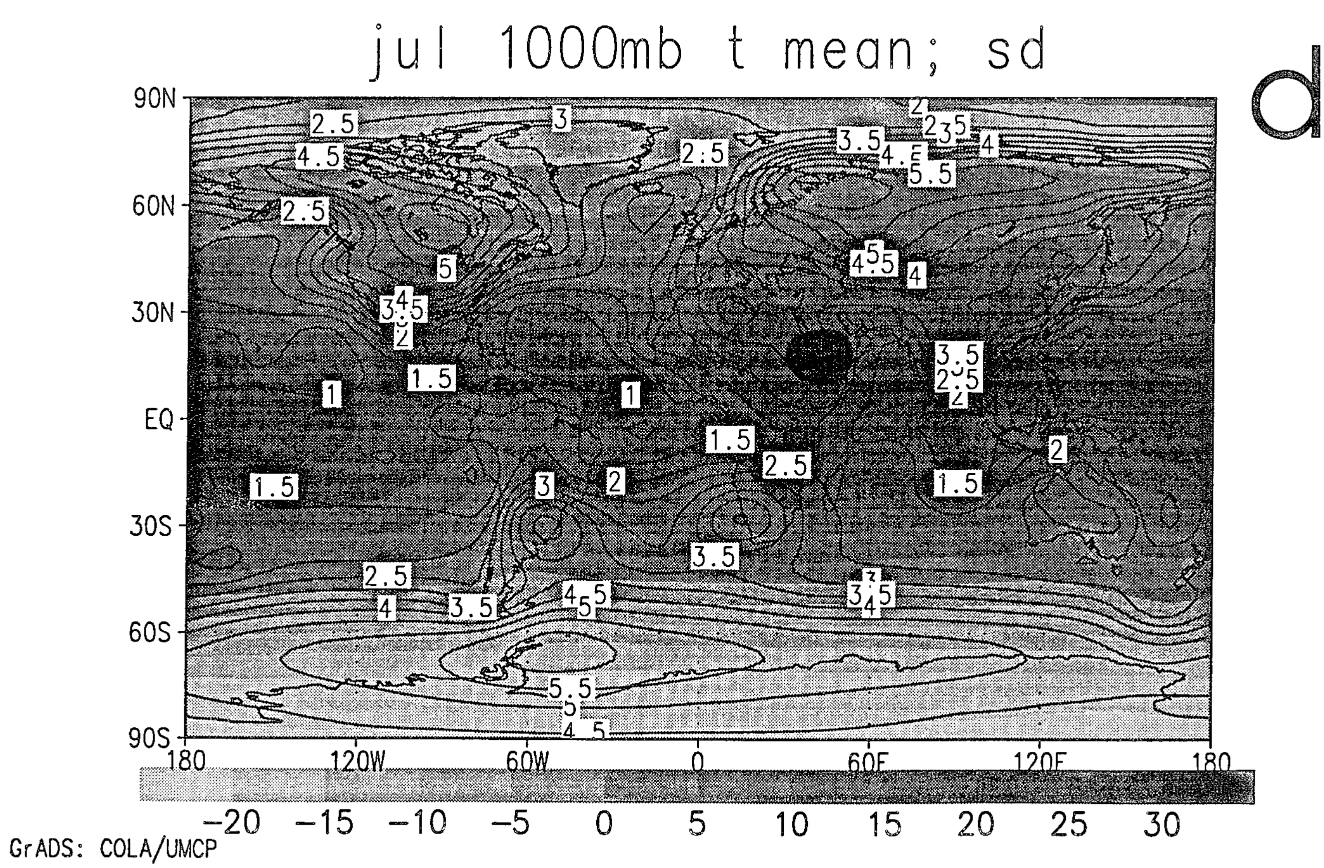

jul 1000mb t mean; sd
d
90N
60N
30N
EQ
30S
60S
90S
180
120W
60W
0
60E
120E
180
−20
−15
−10
−5
0
5
10
15
20
25
30
GrADS: COLA/UMCP

Figure 2

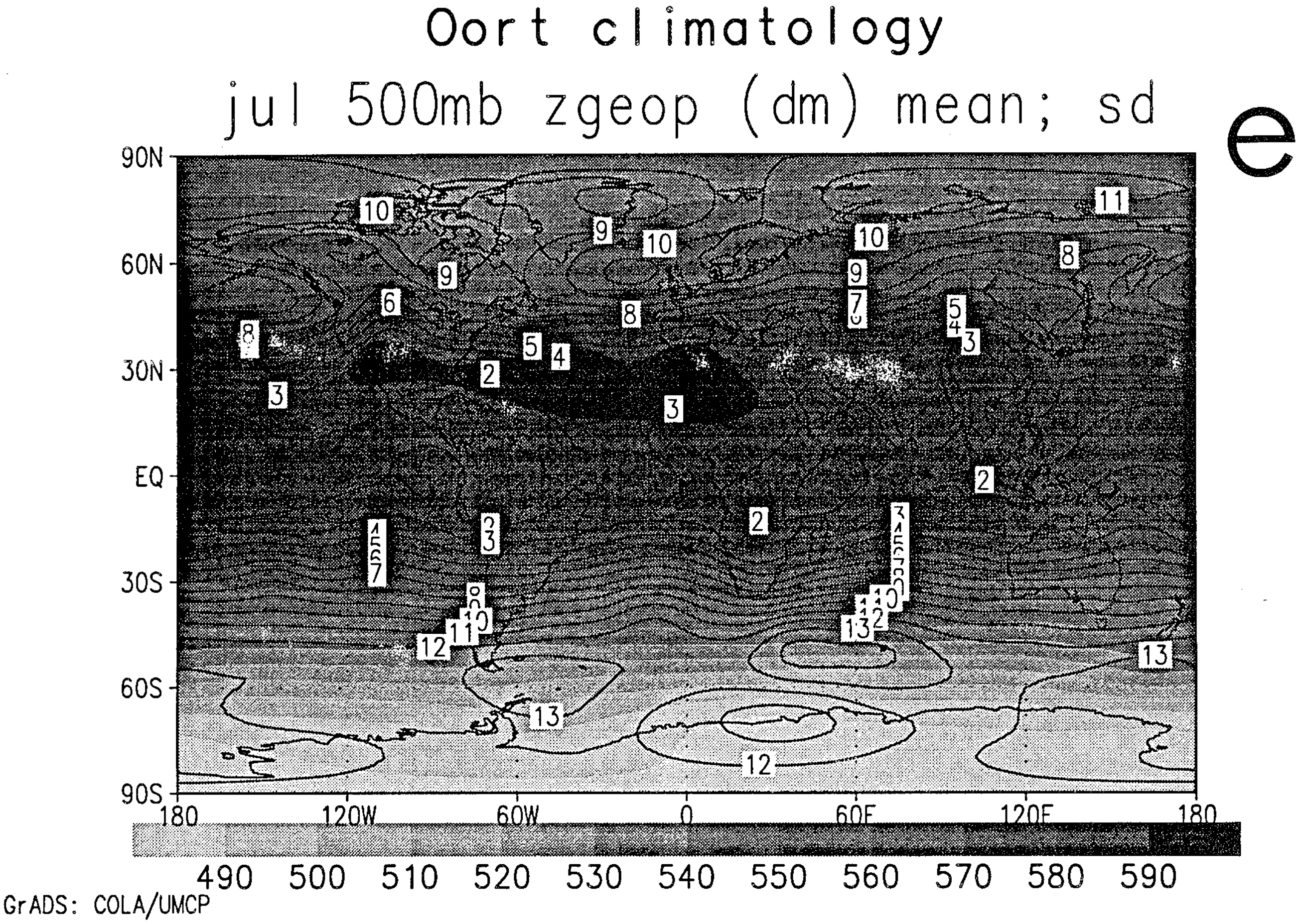

Oort climatology
jul 500mb zgeop (dm) mean; sd
e
90N
60N
30N
EQ
30S
60S
90S
180
120W
60W
0
60E
120E
180
490
500
510
520
530
540
550
560
570
580
590
GrADS: COLA/UMCP

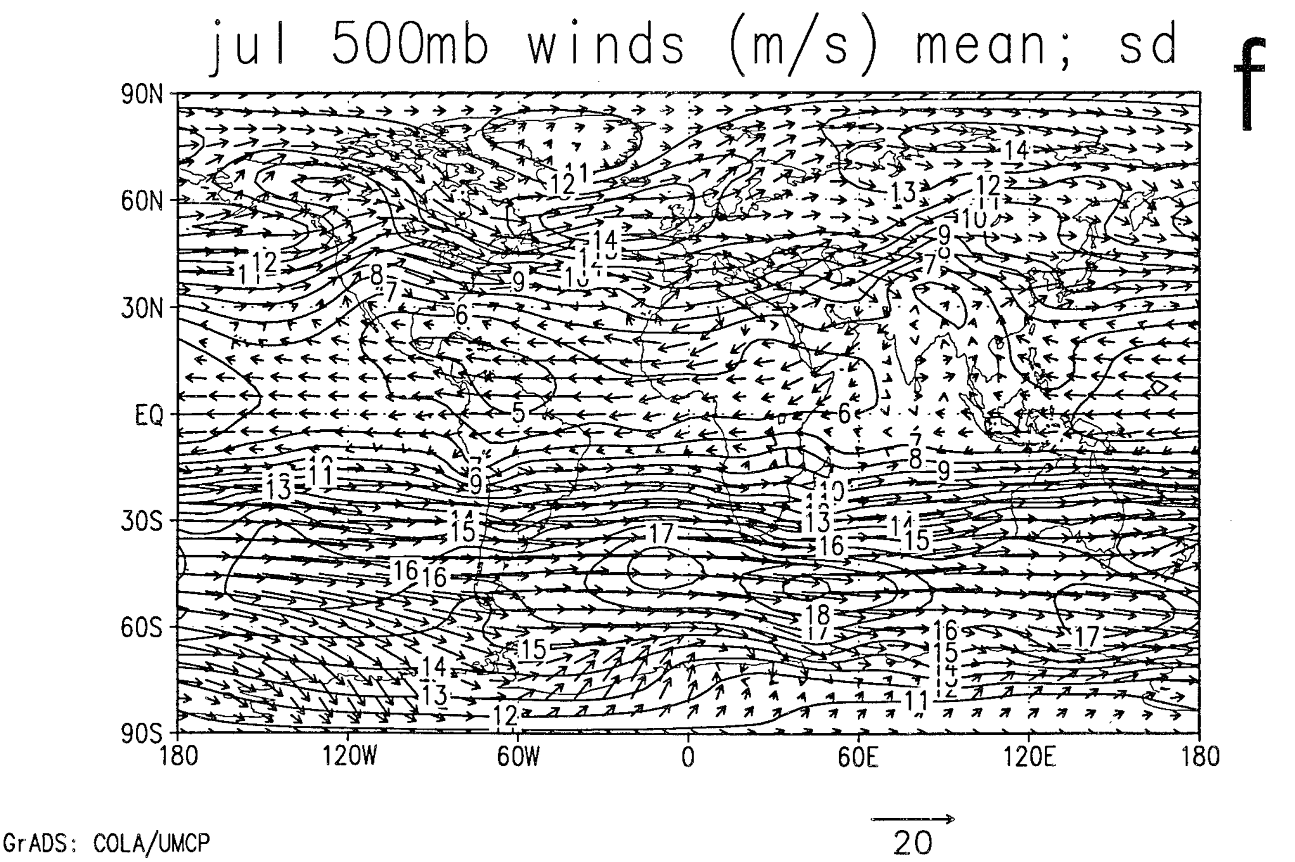

jul 500mb winds (m/s) mean; sd
f
90N
60N
30N
EQ
30S
60S
90S
180
120W
60W
0
60E
120E
180
GrADS: COLA/UMCP
20

Figure 2

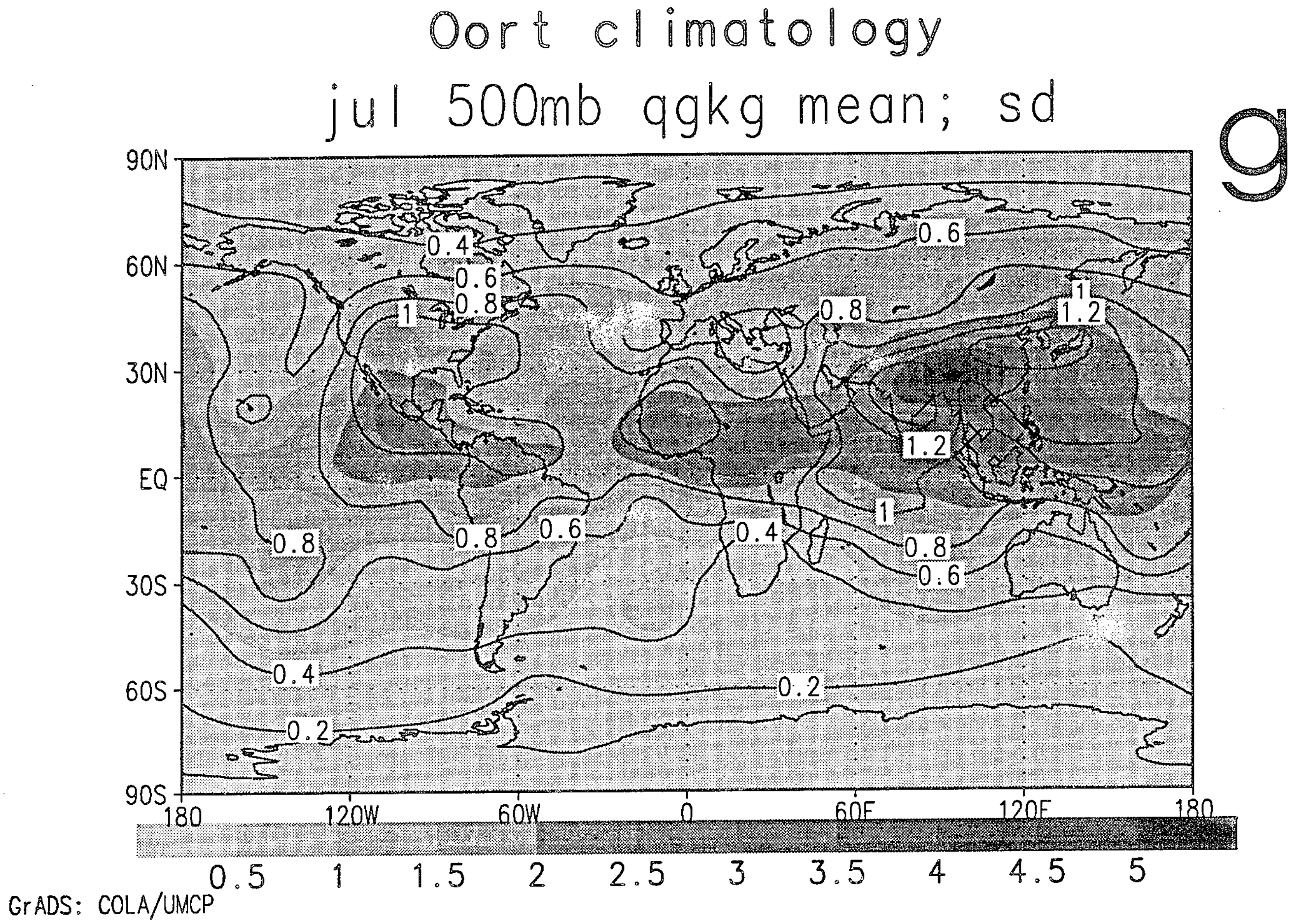
Oort climatology
jul 500mb qgkg mean; sd
g
90N
60N
30N
EQ
30S
60S
90S
180
120W
60W
0
60E
120E
180
0.4
0.6
0.8
1
1.2
0.2
0.5
1.5
2
2.5
3
3.5
4
4.5
5
GrADS: COLA/UMCP

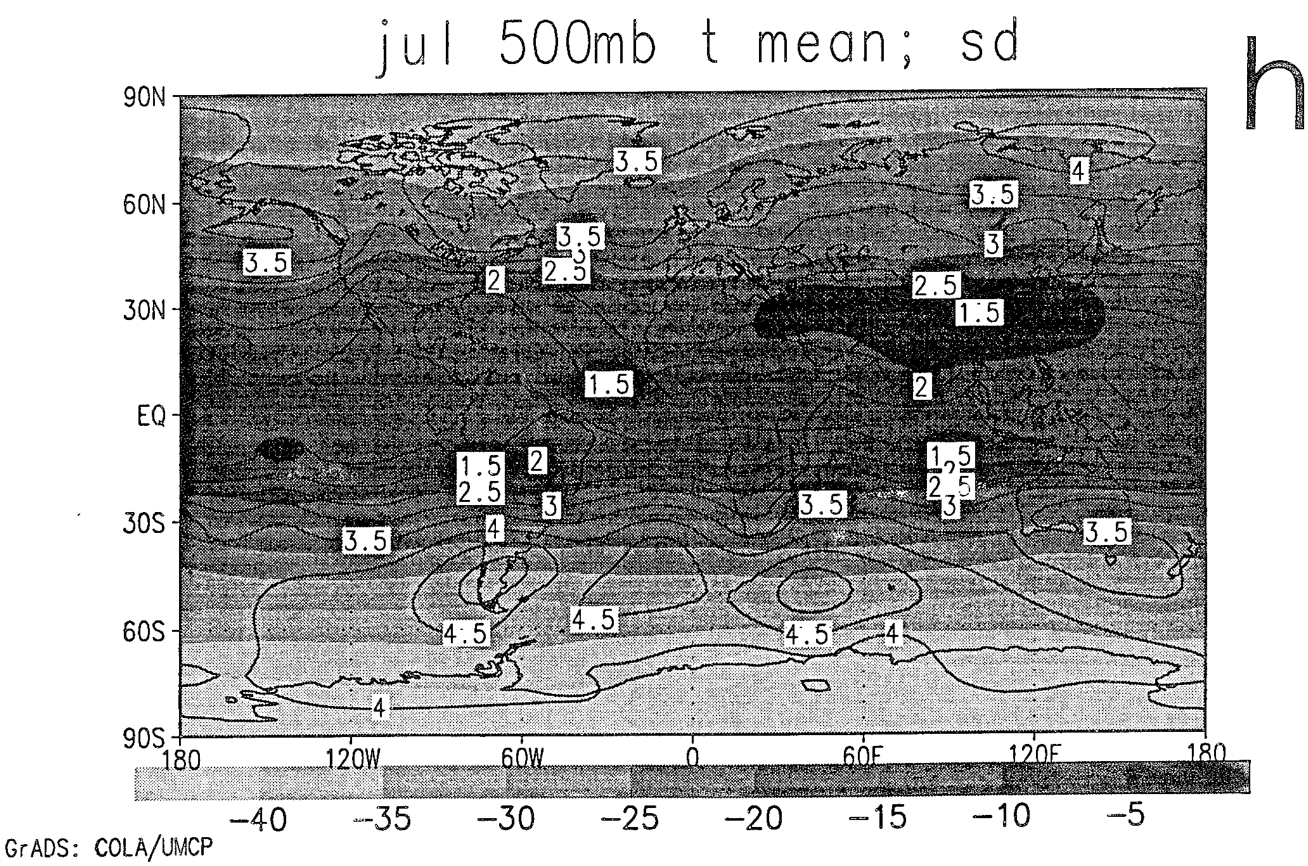
jul 500mb t mean; sd
h
90N
60N
30N
EQ
30S
60S
90S
180
120W
60W
0
60E
120E
180
3.5
4
3
2.5
2
1.5
4.5
−40
−35
−30
−25
−20
−15
−10
−5
GrADS: COLA/UMCP

Figure 2

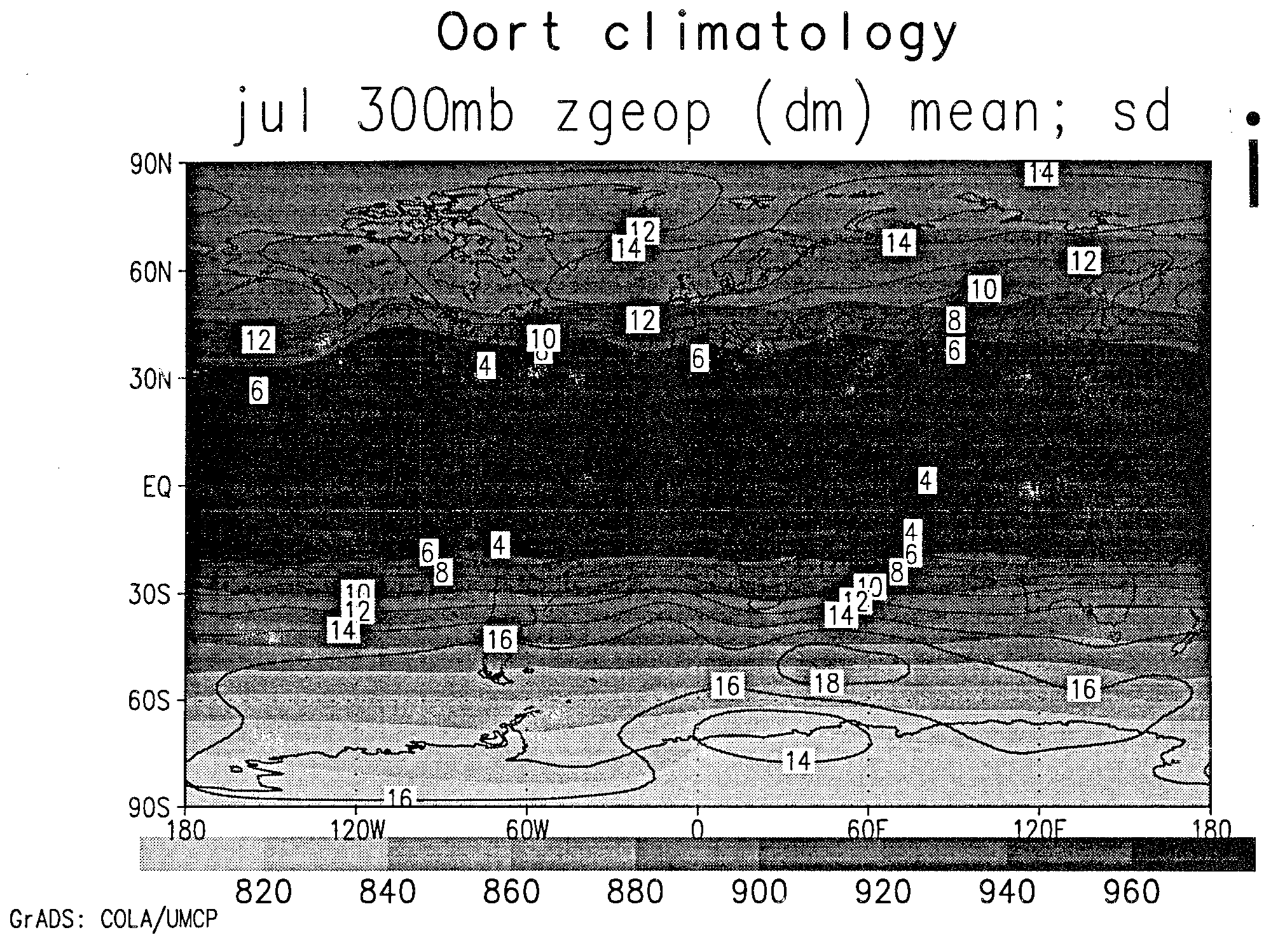
Oort climatology
jul 300mb zgeop (dm) mean; sd
i
90N
60N
30N
EQ
30S
60S
90S
180
120W
60W
0
60E
120E
180
820
840
860
880
900
920
940
960
GrADS: COLA/UMCP

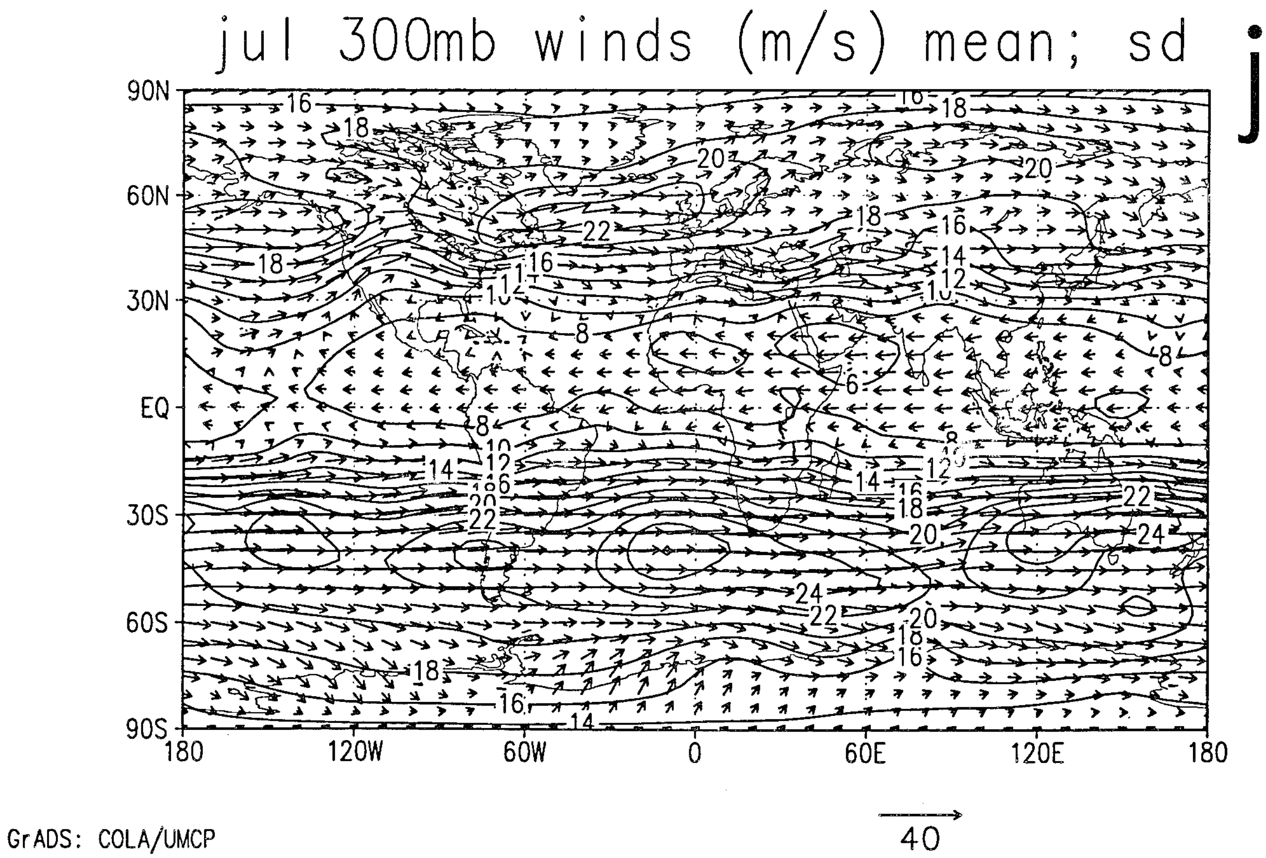
jul 300mb winds (m/s) mean; sd
j
90N
60N
30N
EQ
30S
60S
90S
180
120W
60W
0
60E
120E
180
40
GrADS: COLA/UMCP

Figure 2

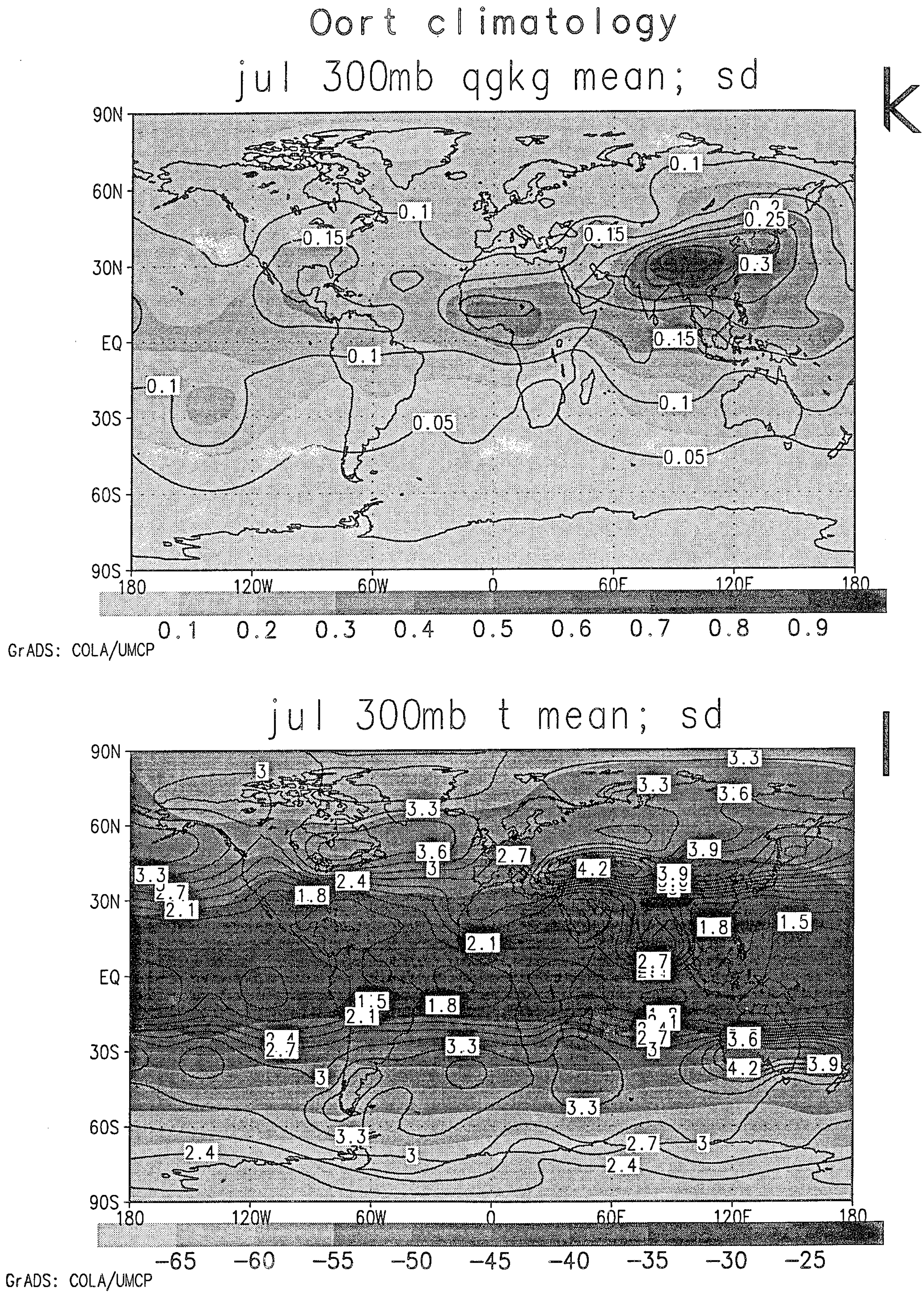
Oort climatology
jul 300mb qgkg mean; sd
90N
60N
30N
EQ
30S
60S
90S
180
120W
60W
0
60E
120E
180
0.1
0.2
0.3
0.4
0.5
0.6
0.7
0.8
0.9
GrADS: COLA/UMCP
jul 300mb t mean; sd
90N
60N
30N
EQ
30S
60S
90S
180
120W
60W
0
60E
120E
180
−65
−60
−55
−50
−45
−40
−35
−30
−25
GrADS: COLA/UMCP

Figure 2

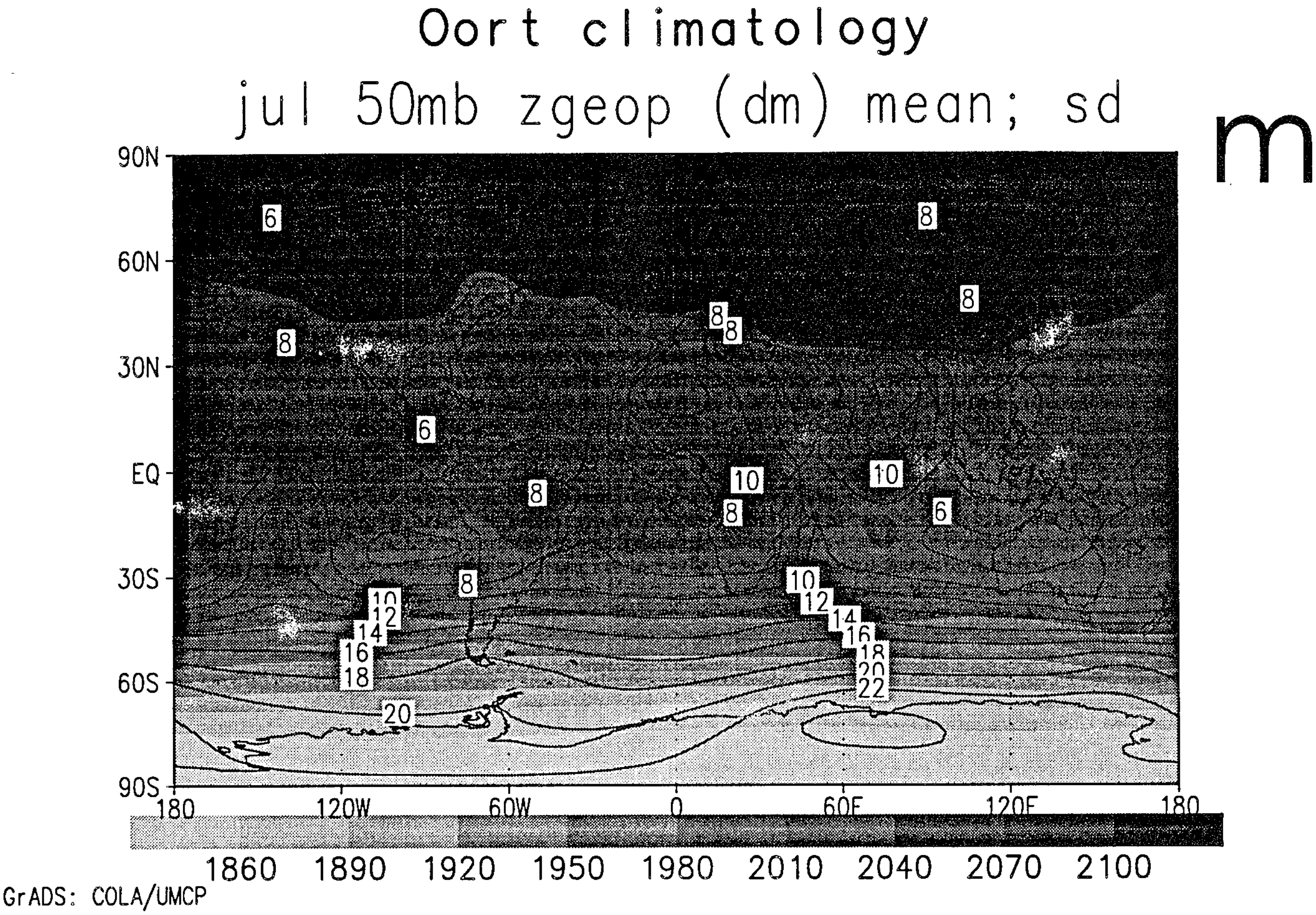

Oort climatology
jul 50mb zgeop (dm) mean; sd
m
90N
60N
30N
EQ
30S
60S
90S
180
120W
60W
0
60E
120E
180
1860
1890
1920
1950
1980
2010
2040
2070
2100
GrADS: COLA/UMCP

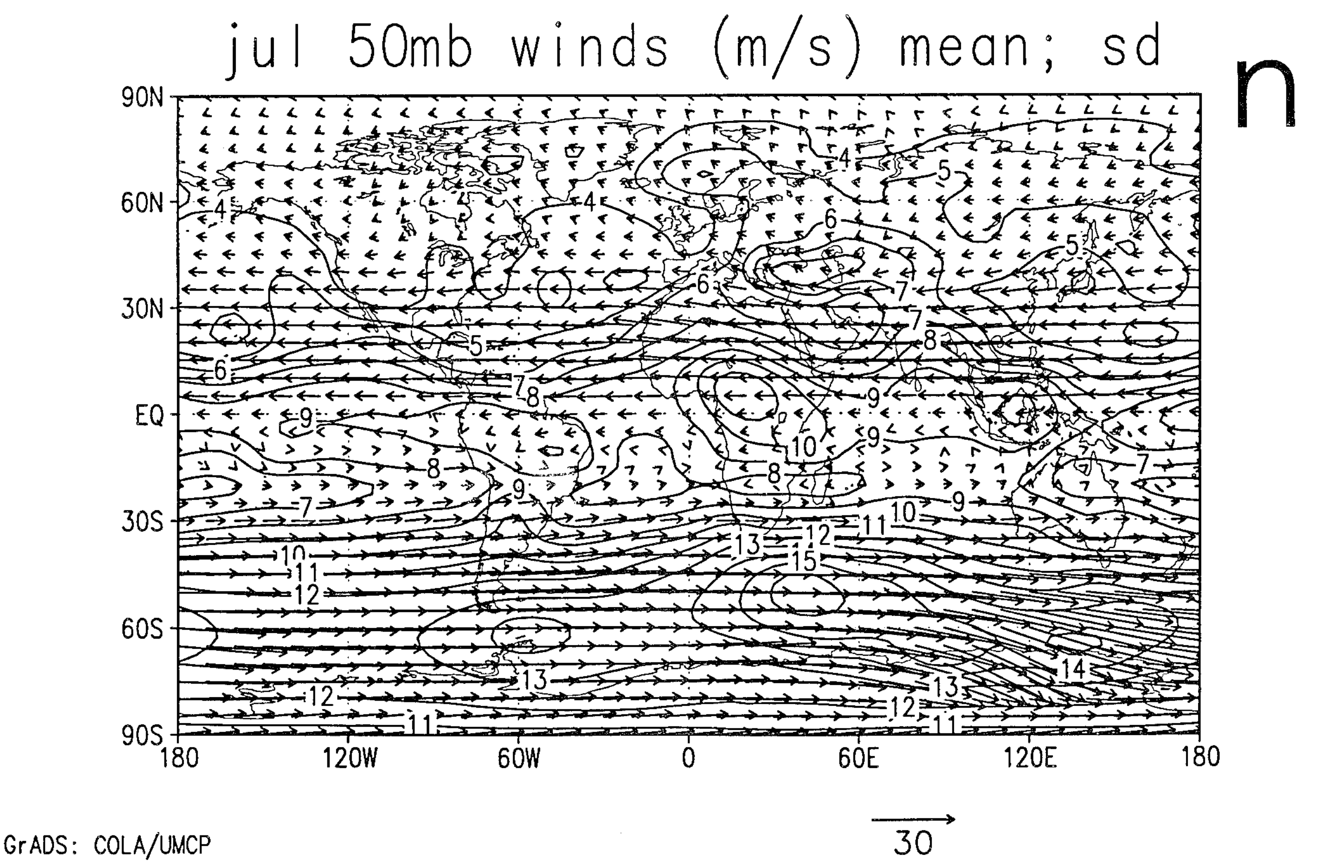

jul 50mb winds (m/s) mean; sd
n
90N
60N
30N
EQ
30S
60S
90S
180
120W
60W
0
60E
120E
180
GrADS: COLA/UMCP
30

Figure 3

Oort climatology

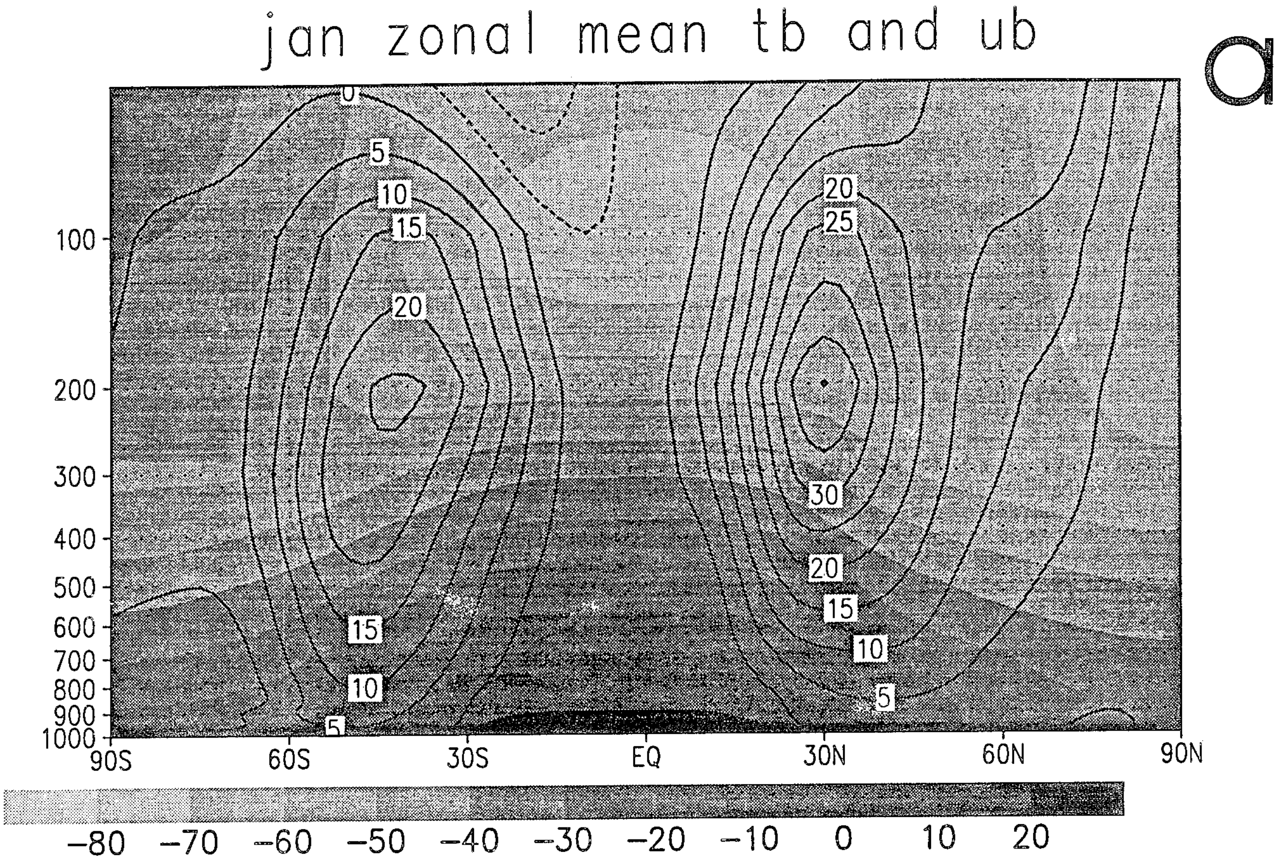

GrADS: COLA/UMCP

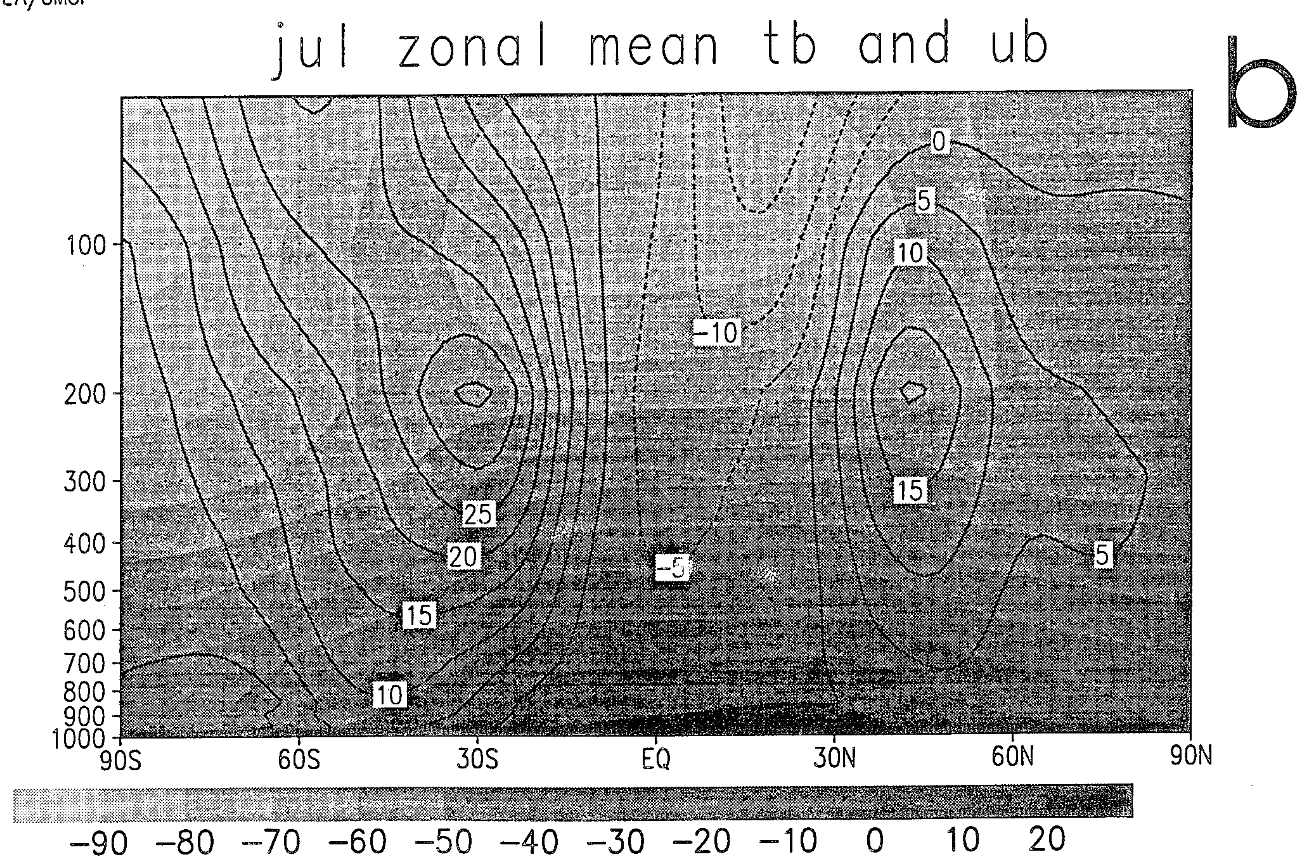

GrADS: COLA/UMCP

Figure 4

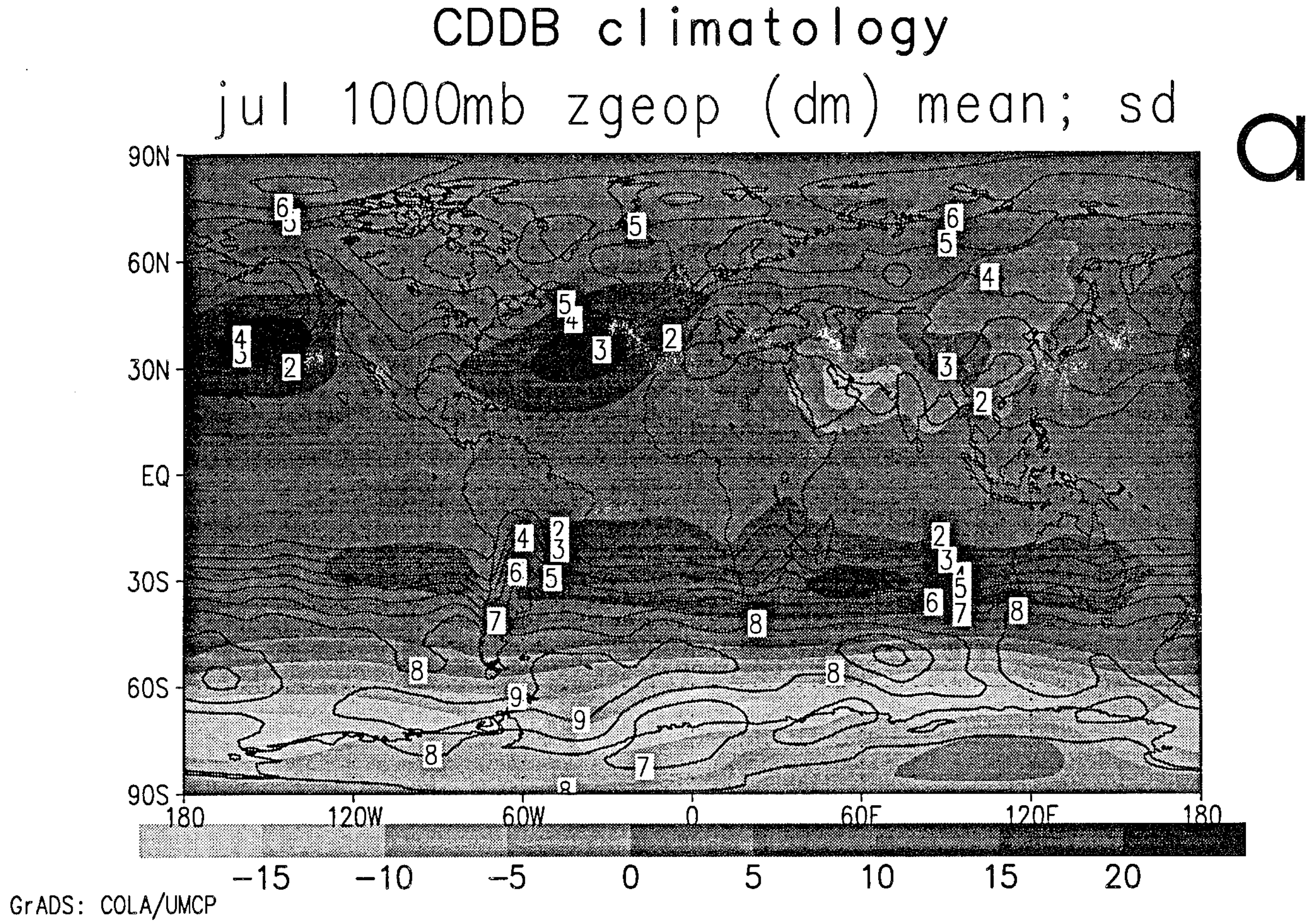
CDDB climatology
jul 1000mb zgeop (dm) mean; sd
a
90N
60N
30N
EQ
30S
60S
90S
180
120W
60W
0
60E
120E
180
−15
−10
−5
0
5
10
15
20
GrADS: COLA/UMCP

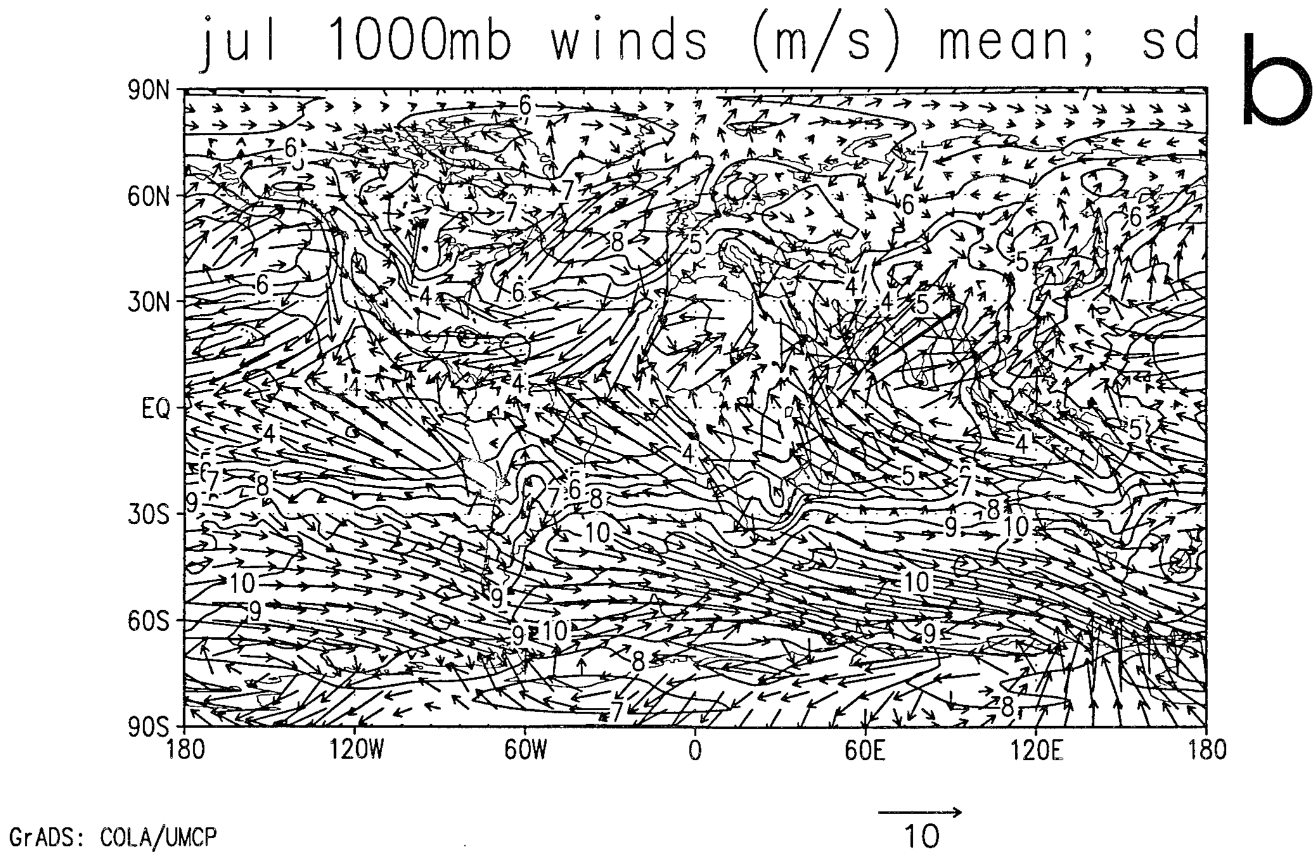
jul 1000mb winds (m/s) mean; sd
b
90N
60N
30N
EQ
30S
60S
90S
180
120W
60W
0
60E
120E
180
10
GrADS: COLA/UMCP

Figure 4

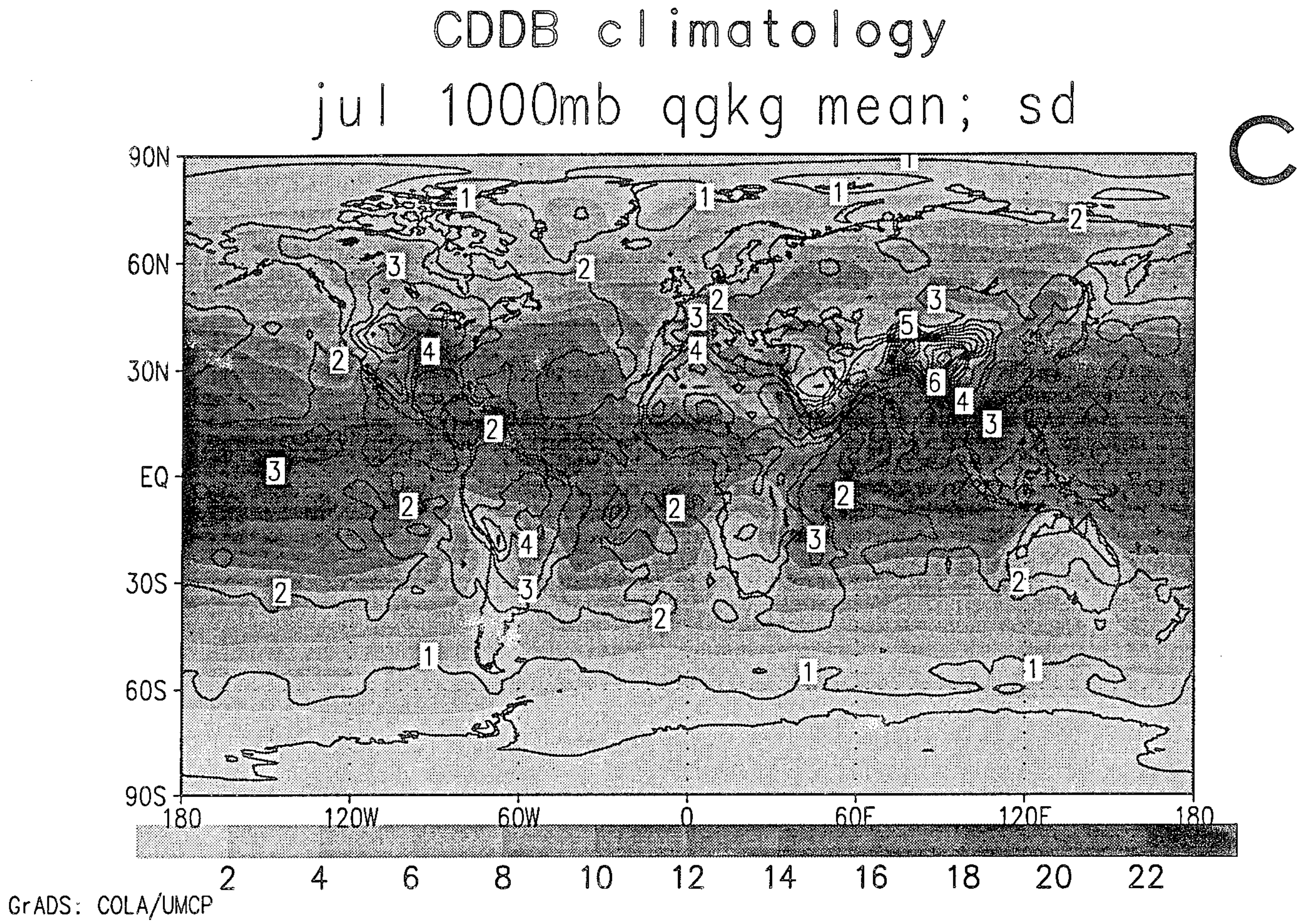
CDDB climatology
jul 1000mb qgkg mean; sd
c
90N
60N
30N
EQ
30S
60S
90S
180
120W
60W
0
60E
120E
180
2 4 6 8 10 12 14 16 18 20 22
GrADS: COLA/UMCP

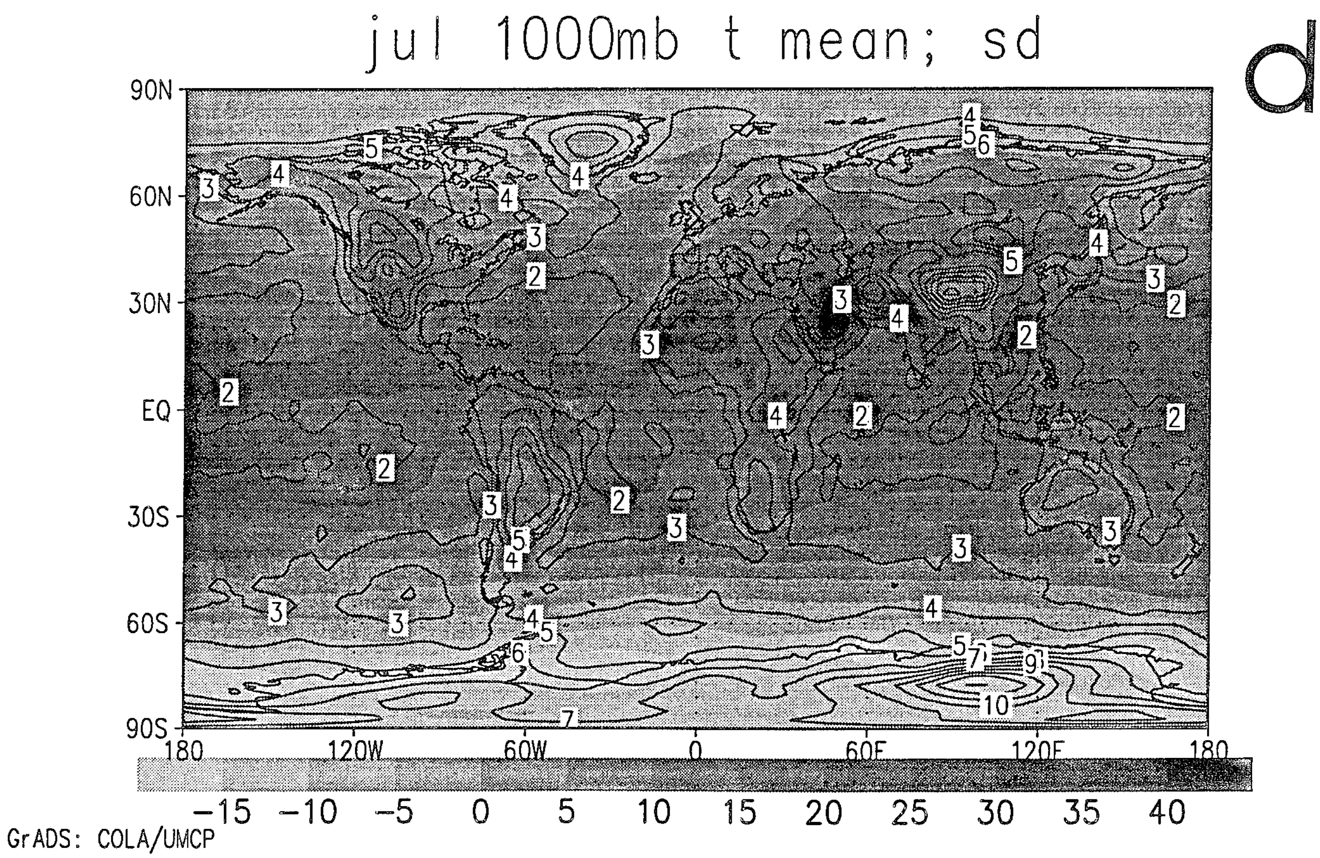
jul 1000mb t mean; sd
d
90N
60N
30N
EQ
30S
60S
90S
180
120W
60W
0
60E
120E
180
−15 −10 −5 0 5 10 15 20 25 30 35 40
GrADS: COLA/UMCP

Figure 4

CDDB climatology

jul 500mb zgeop (dm) mean; sd

e

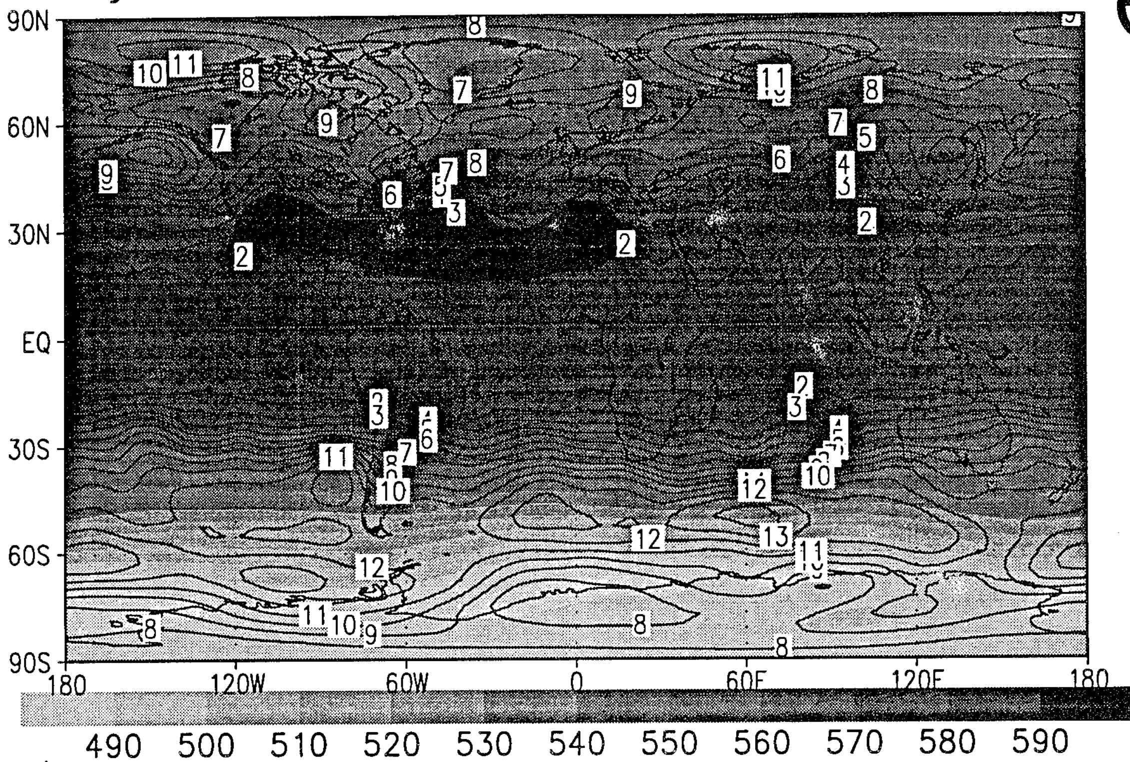

GrADS: COLA/UMCP

jul 500mb winds (m/s) mean; sd

f

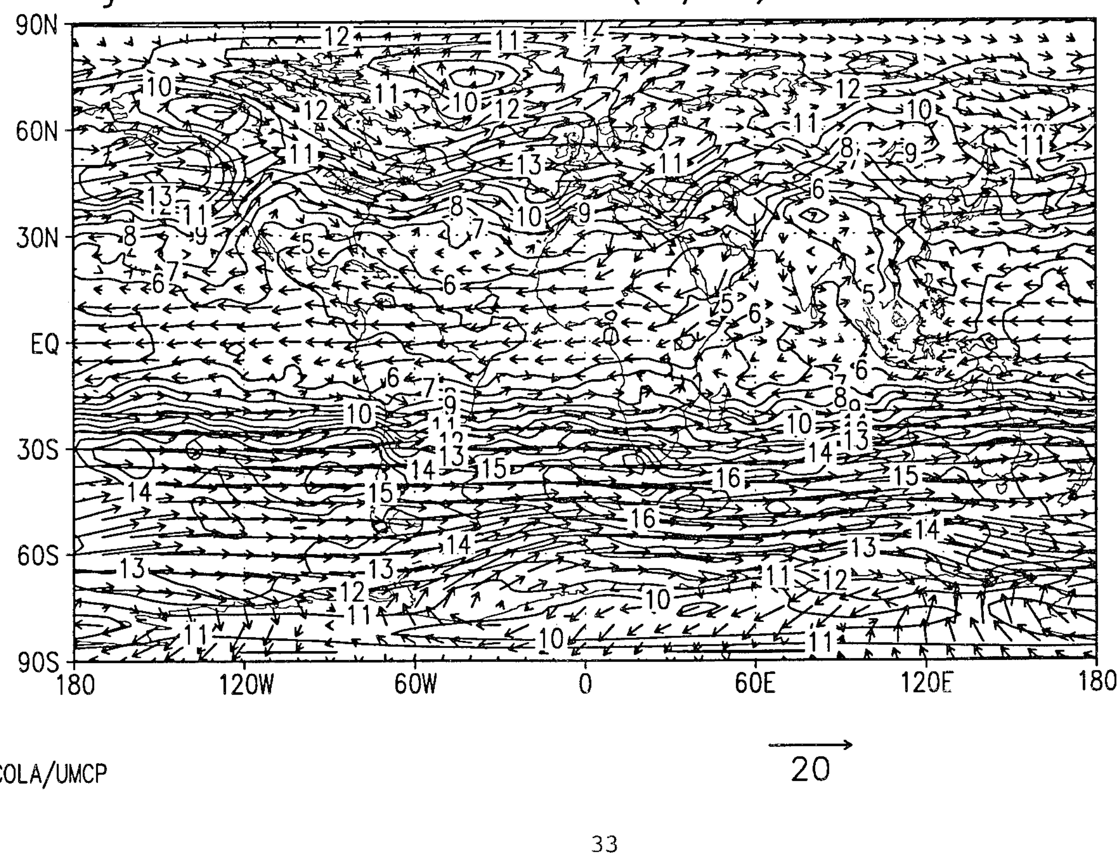

GrADS: COLA/UMCP

Figure 4

CDDB climatology

jul 500mb qgkg mean; sd

g

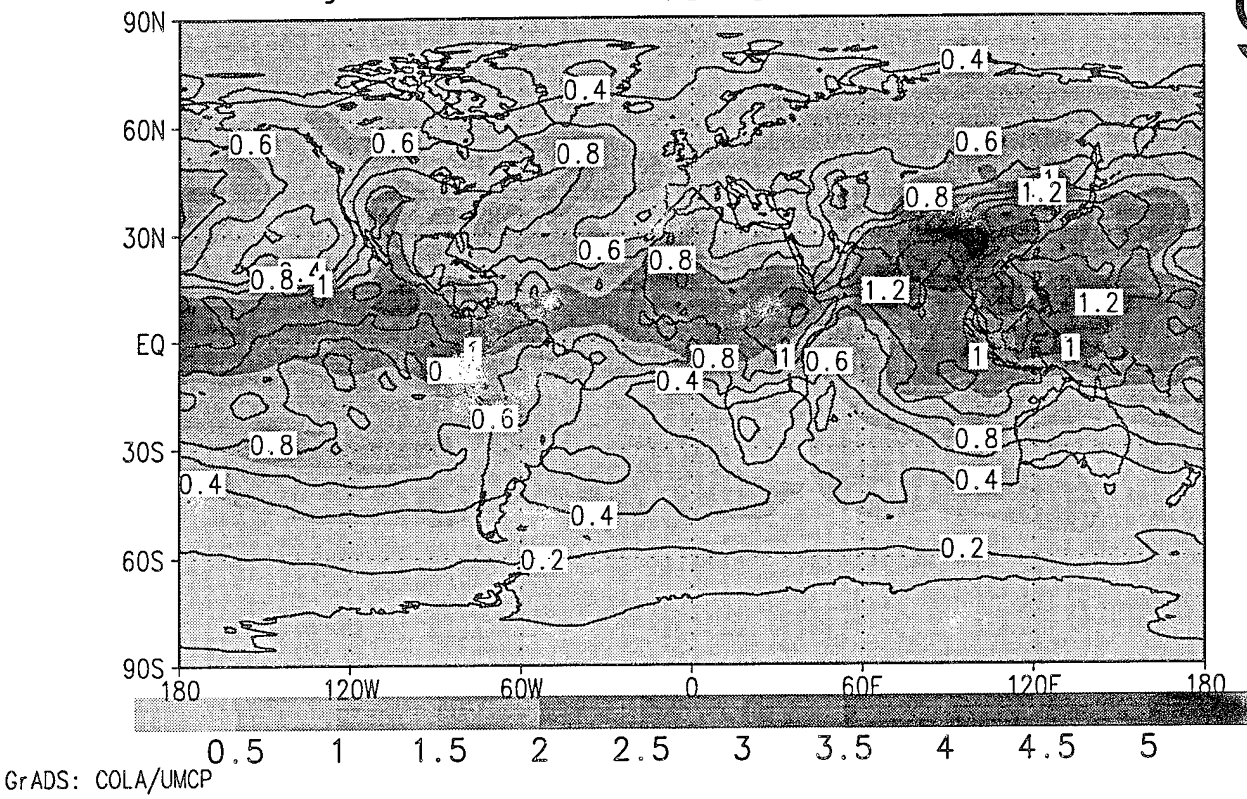

jul 500mb t mean; sd

h

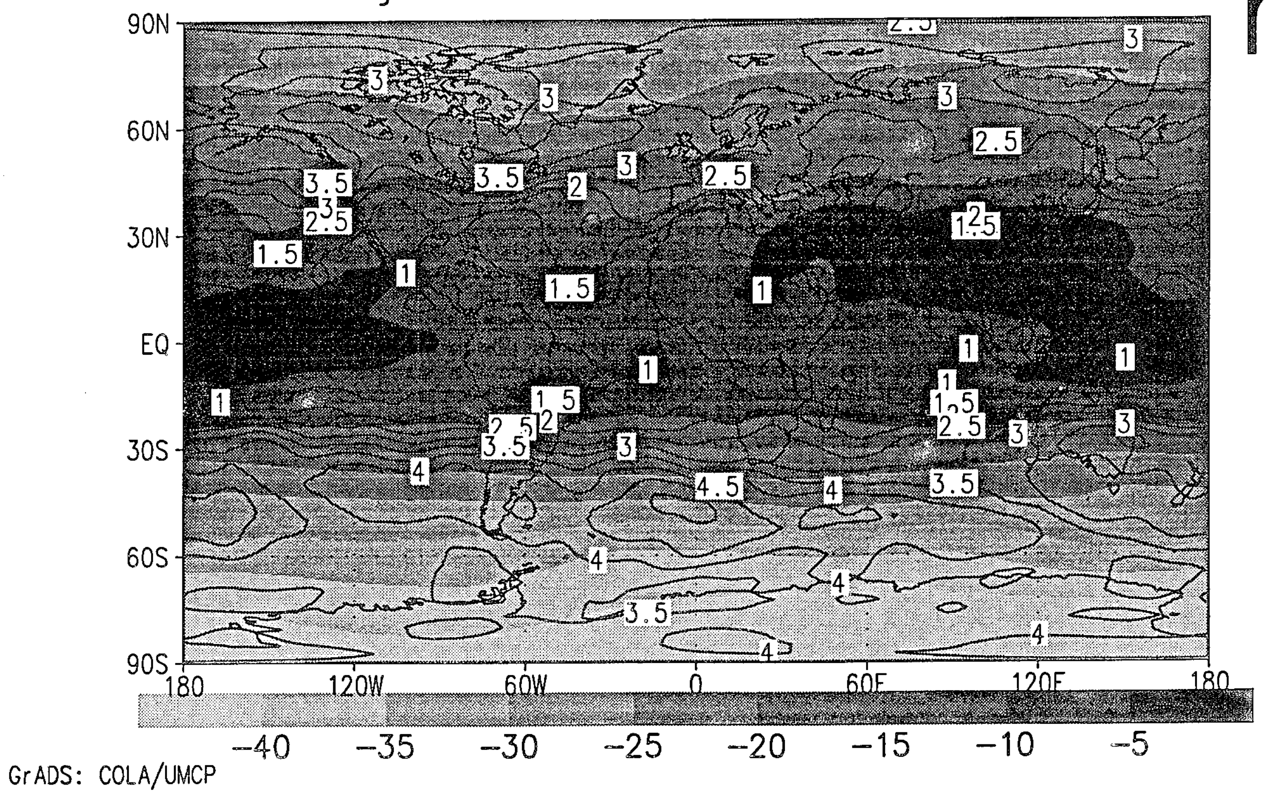

Figure 4

CDDB climatology

jul 300mb zgeop (dm) mean; sd

i

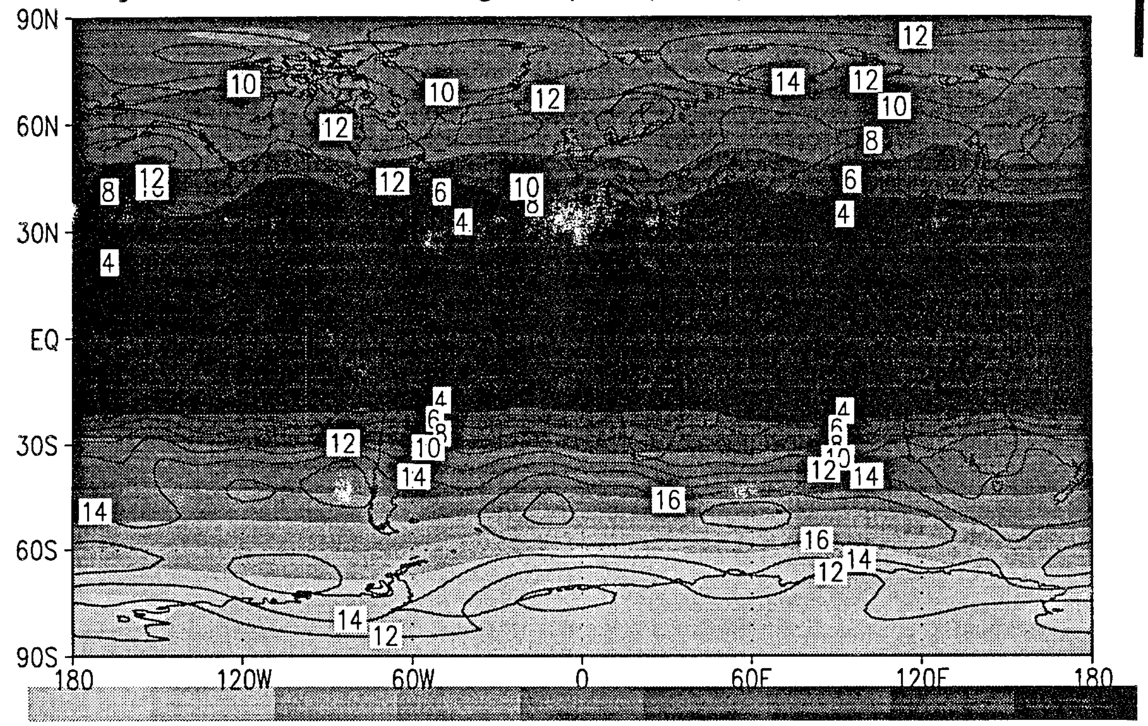

GrADS: COLA/UMCP

jul 300mb winds (m/s) mean; sd

j

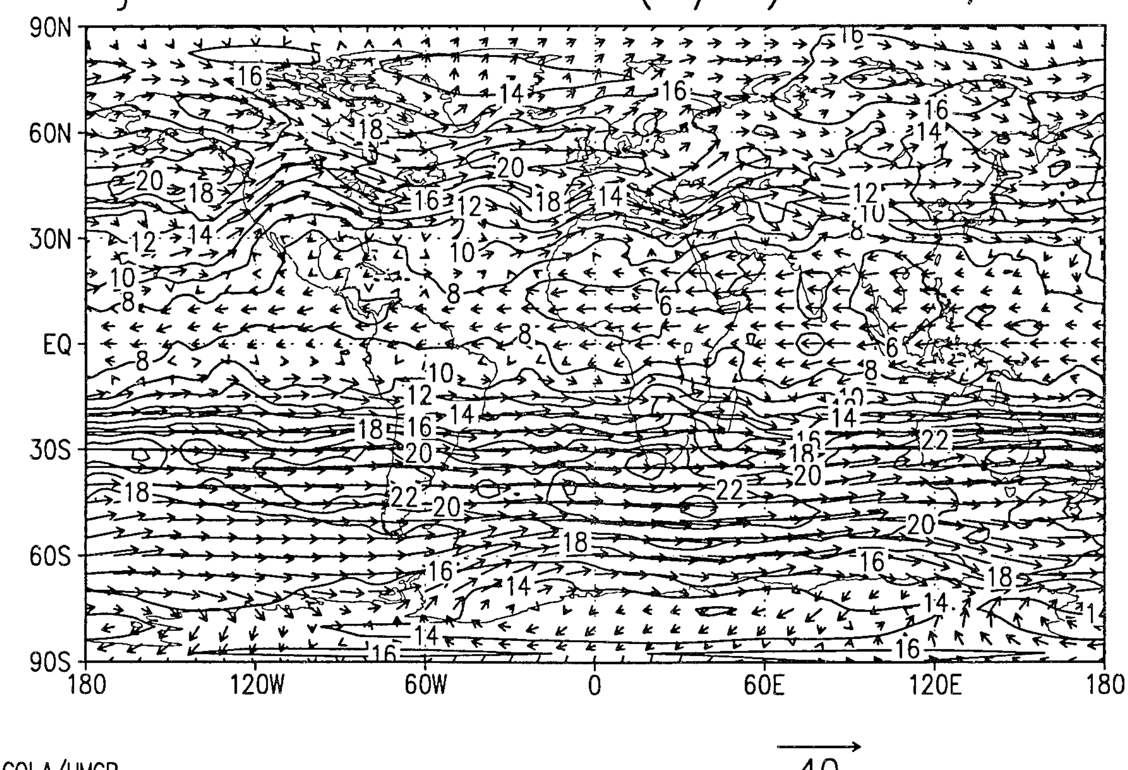

GrADS: COLA/UMCP

Figure 4

CDDB climatology

jul 50mb zgeop (dm) mean; sd

K

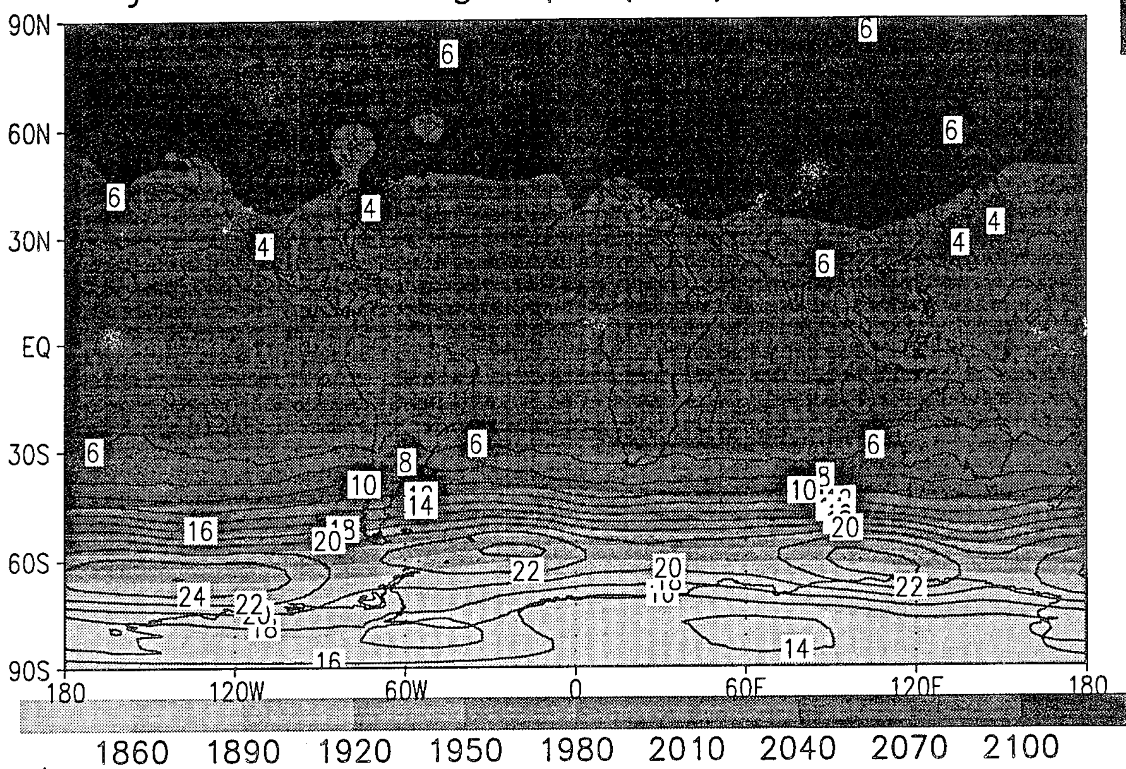

GrADS: COLA/UMCP

jul 50mb winds (m/s) mean; sd

l

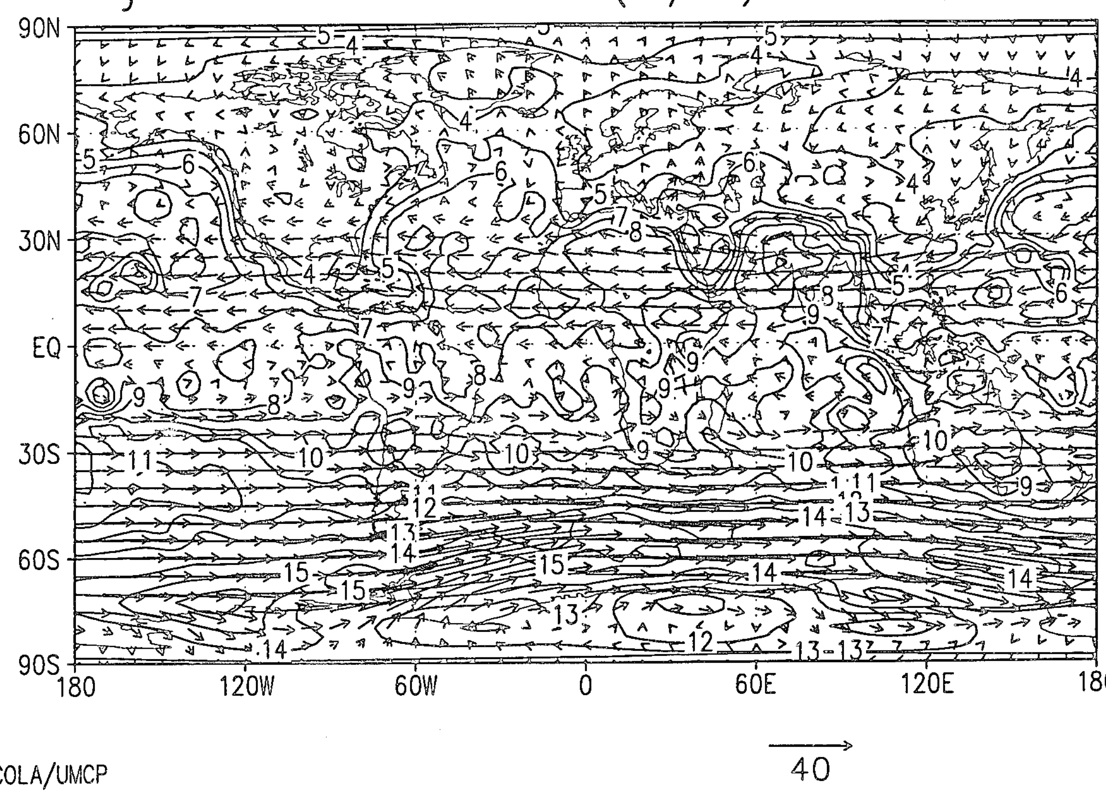

GrADS: COLA/UMCP

Figure 5

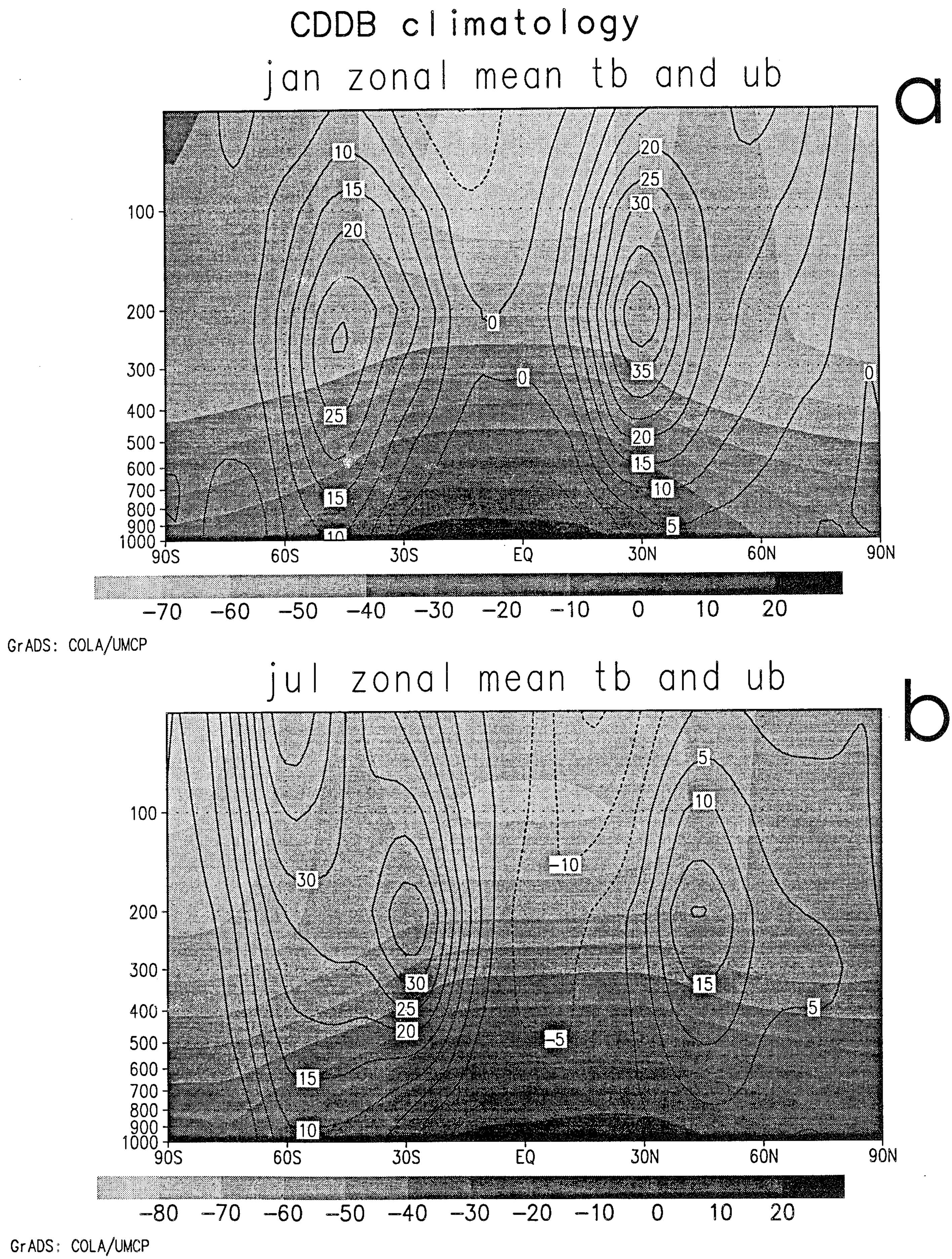

CDDB climatology
jan zonal mean tb and ub
a
100
200
300
400
500
600
700
800
900
1000
90S
60S
30S
EQ
30N
60N
90N
10
15
20
25
30
35
0
5
−70 −60 −50 −40 −30 −20 −10 0 10 20
GrADS: COLA/UMCP
jul zonal mean tb and ub
b
−10
−5
−80 −70 −60 −50 −40 −30 −20 −10 0 10 20
GrADS: COLA/UMCP

ETA 12-hr fcst of 850 hPa height

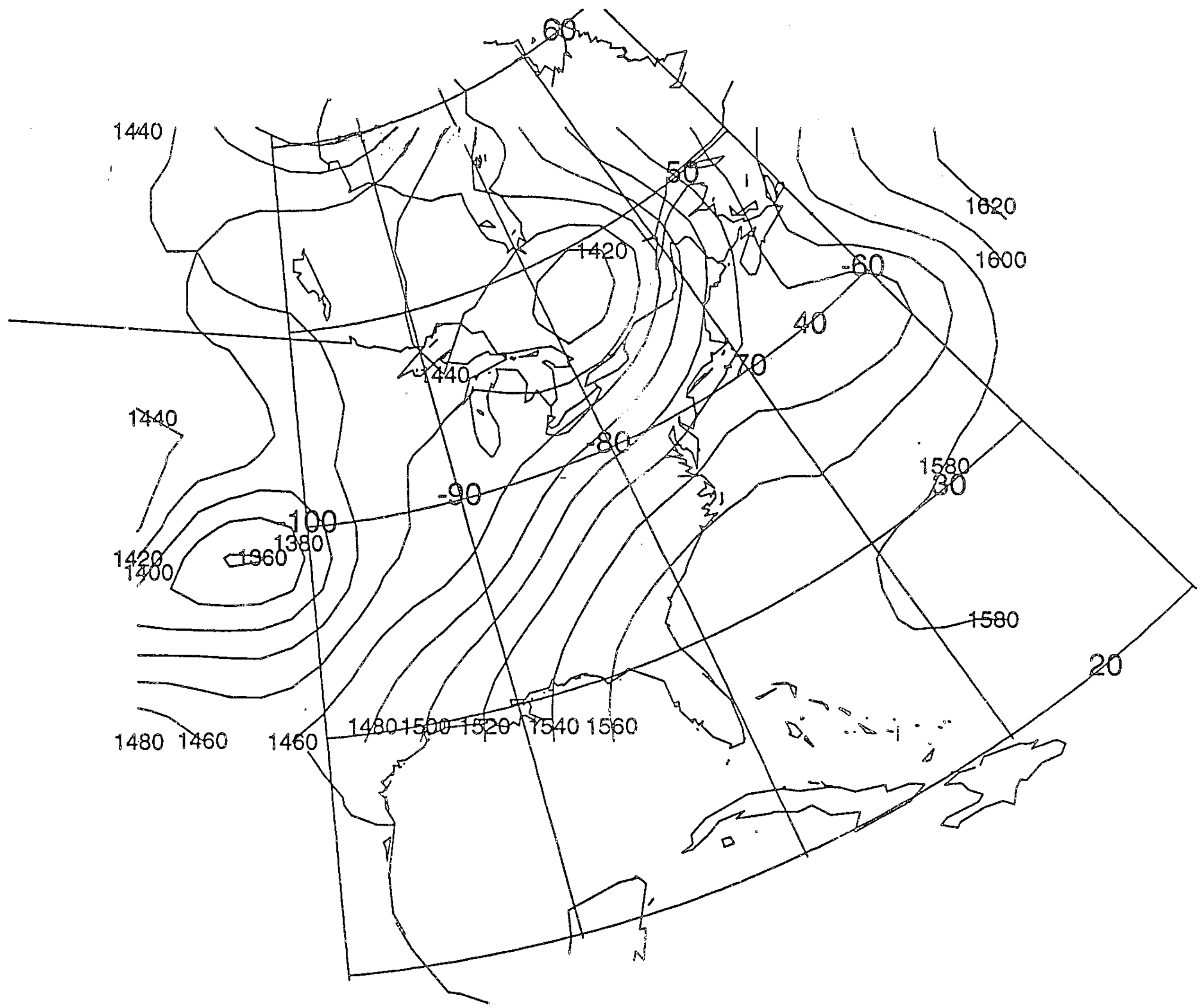

12 UTC 6 March 1995

Figure 6a

ETA background on analysis grid

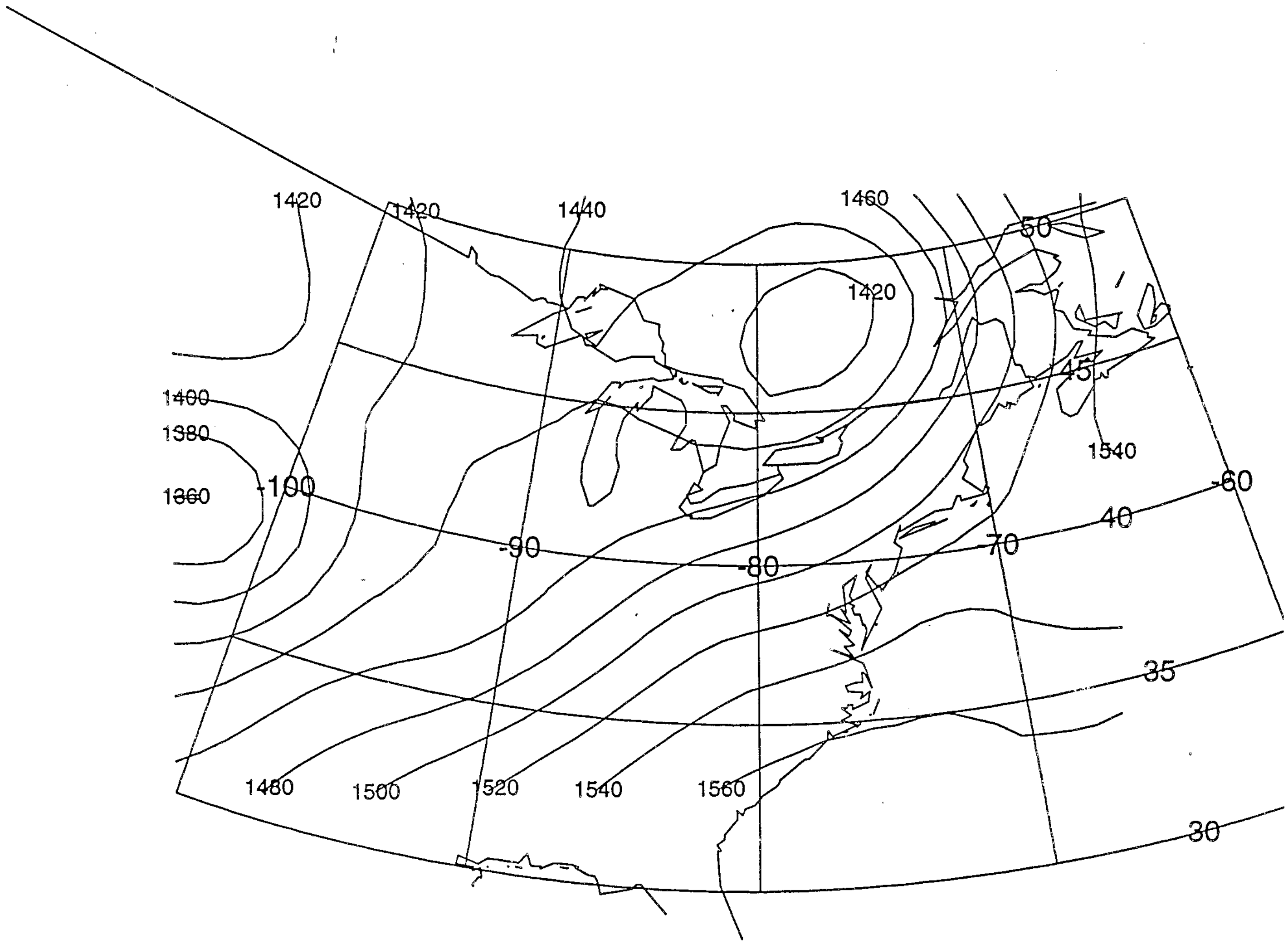

Figure 6b

ETA-Analysis and Raob values

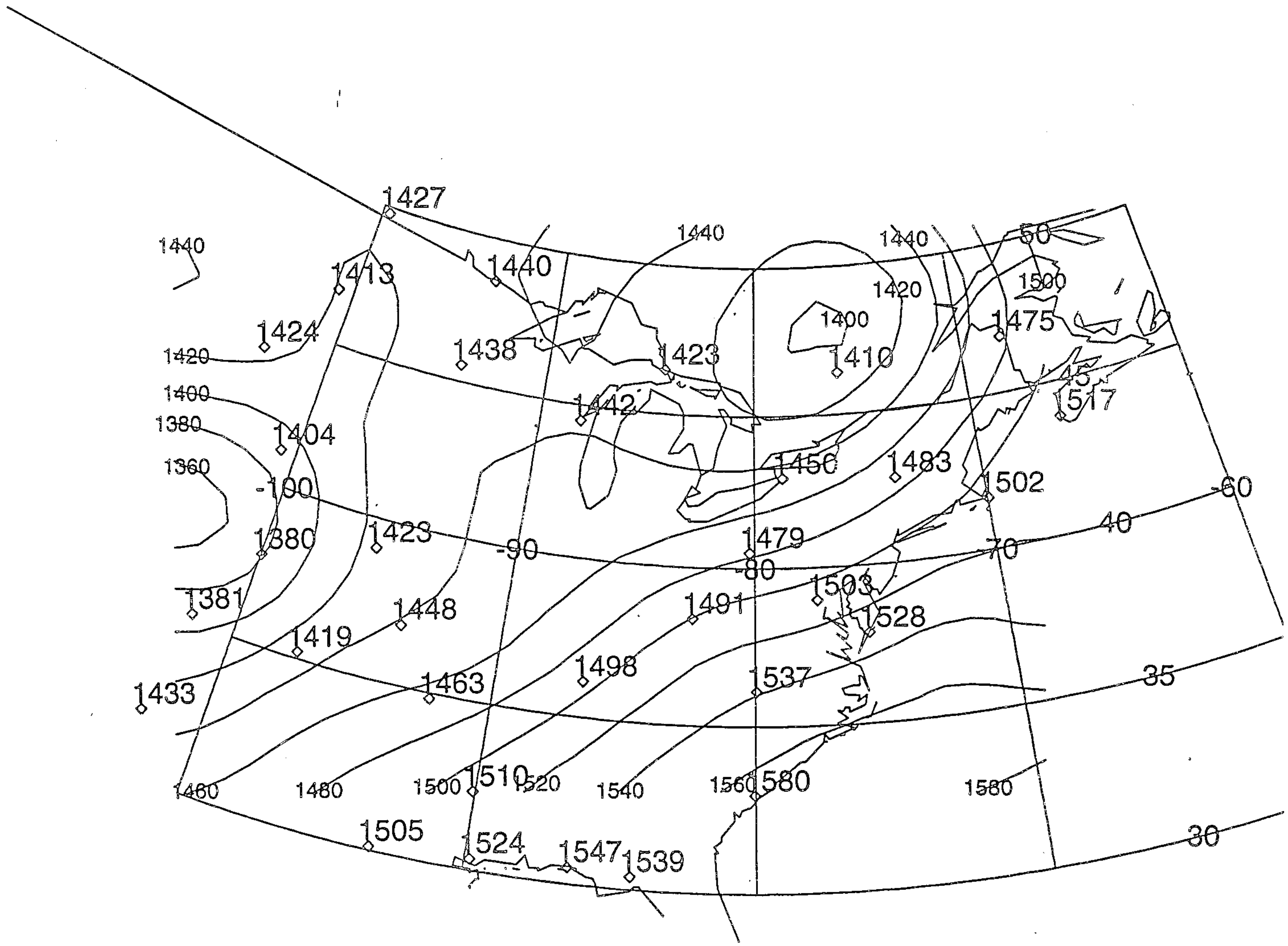

12 UTC 6 Mar 1995

Figure 6c

Analysis Increments

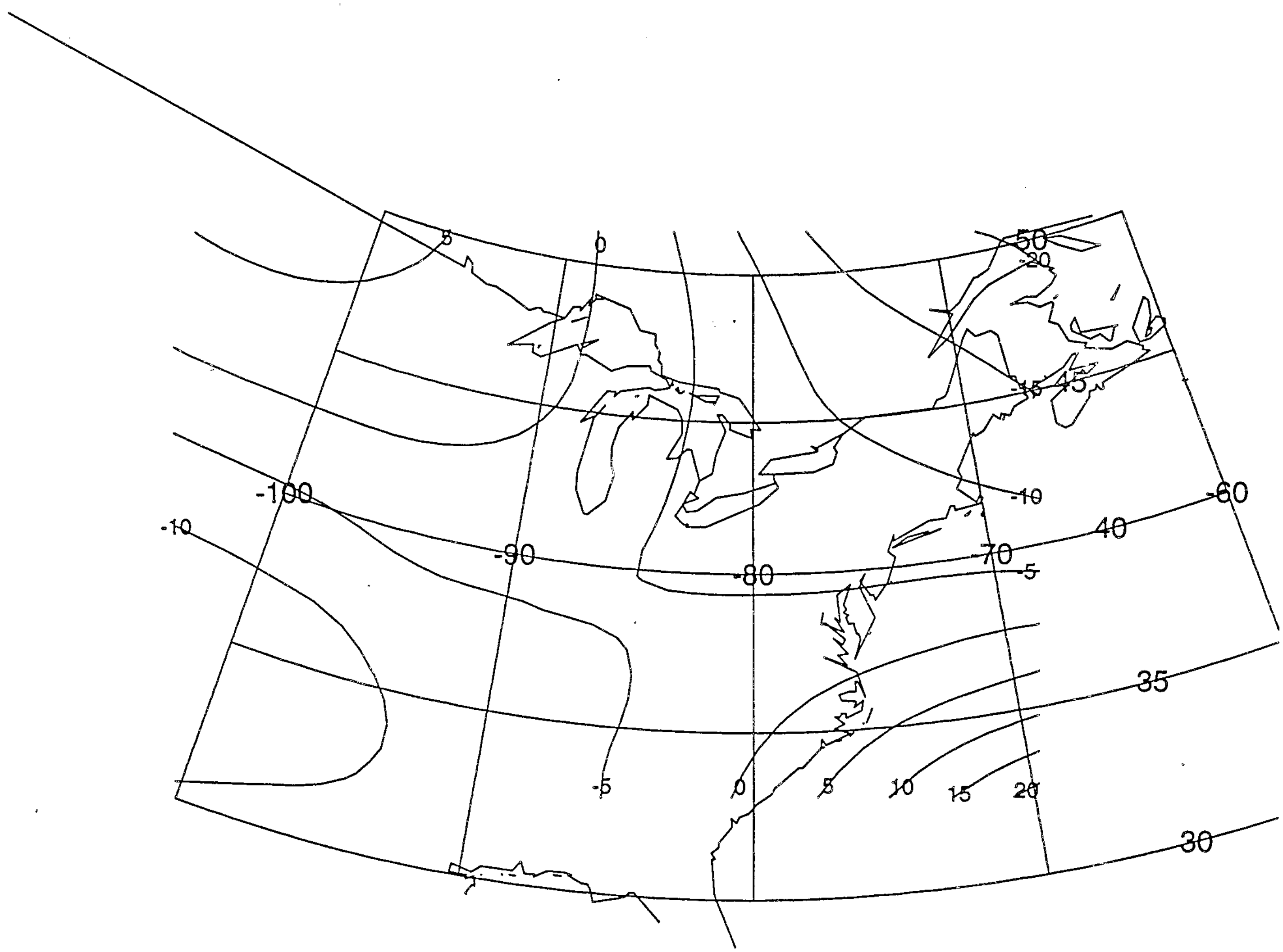

Figure 6d

Climatology of Mar 850 hPa height

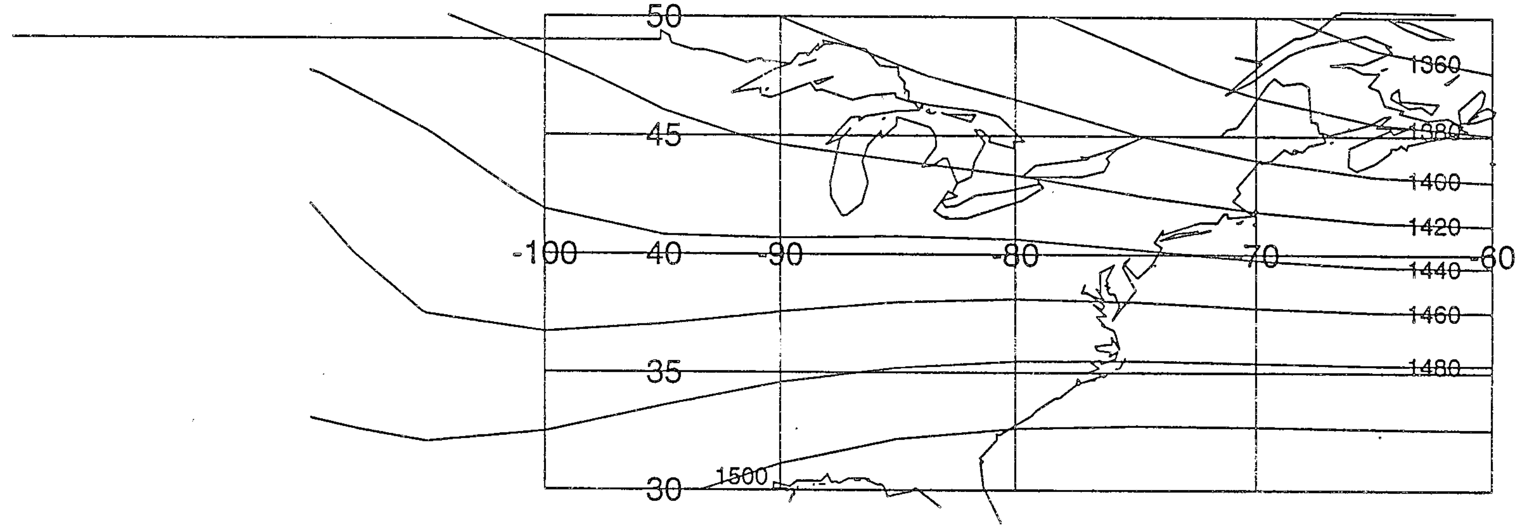

Figure 7a

Climatology background on analysis grid

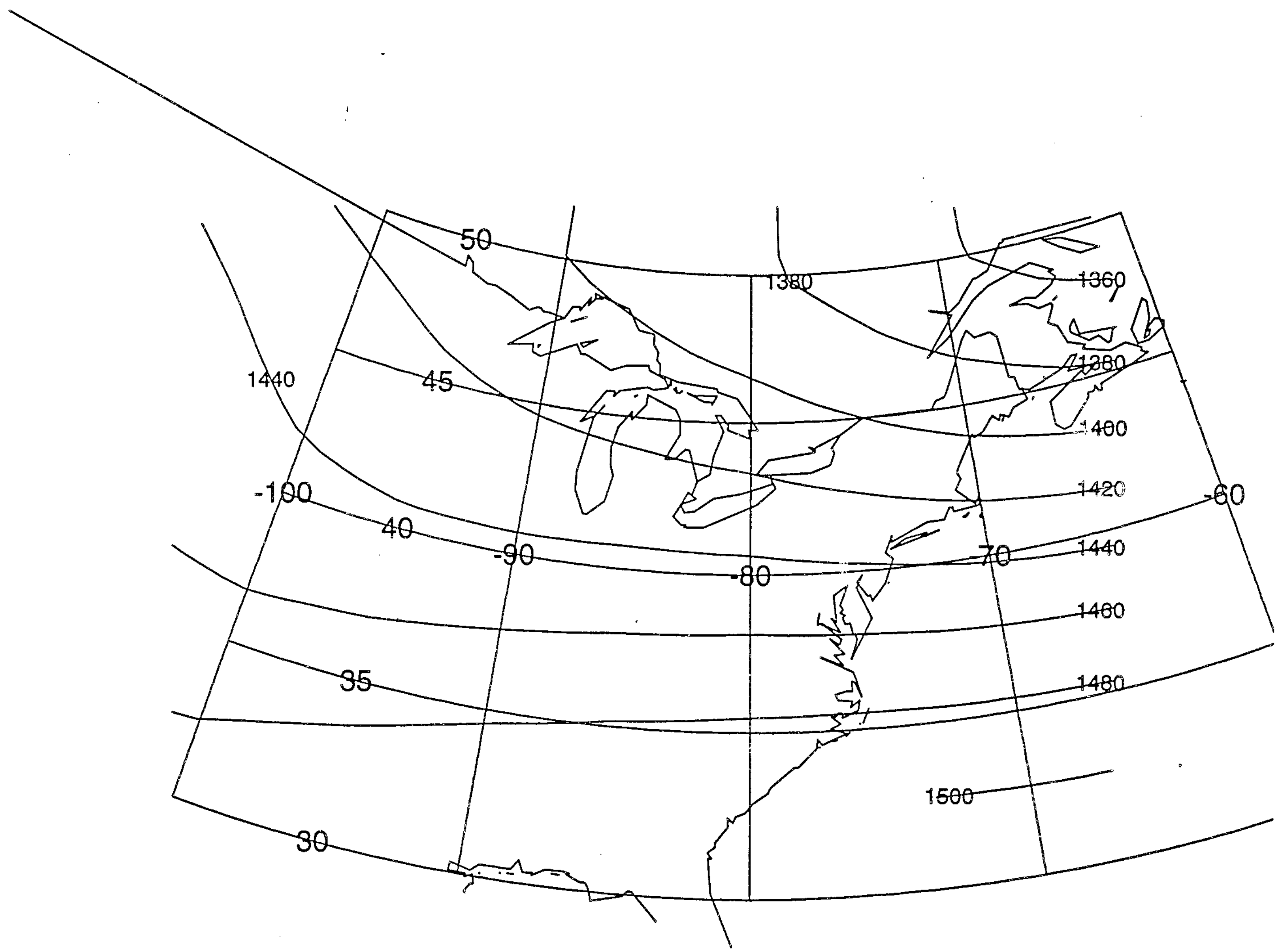

Figure 7b

Cli-Analysis and Raob values

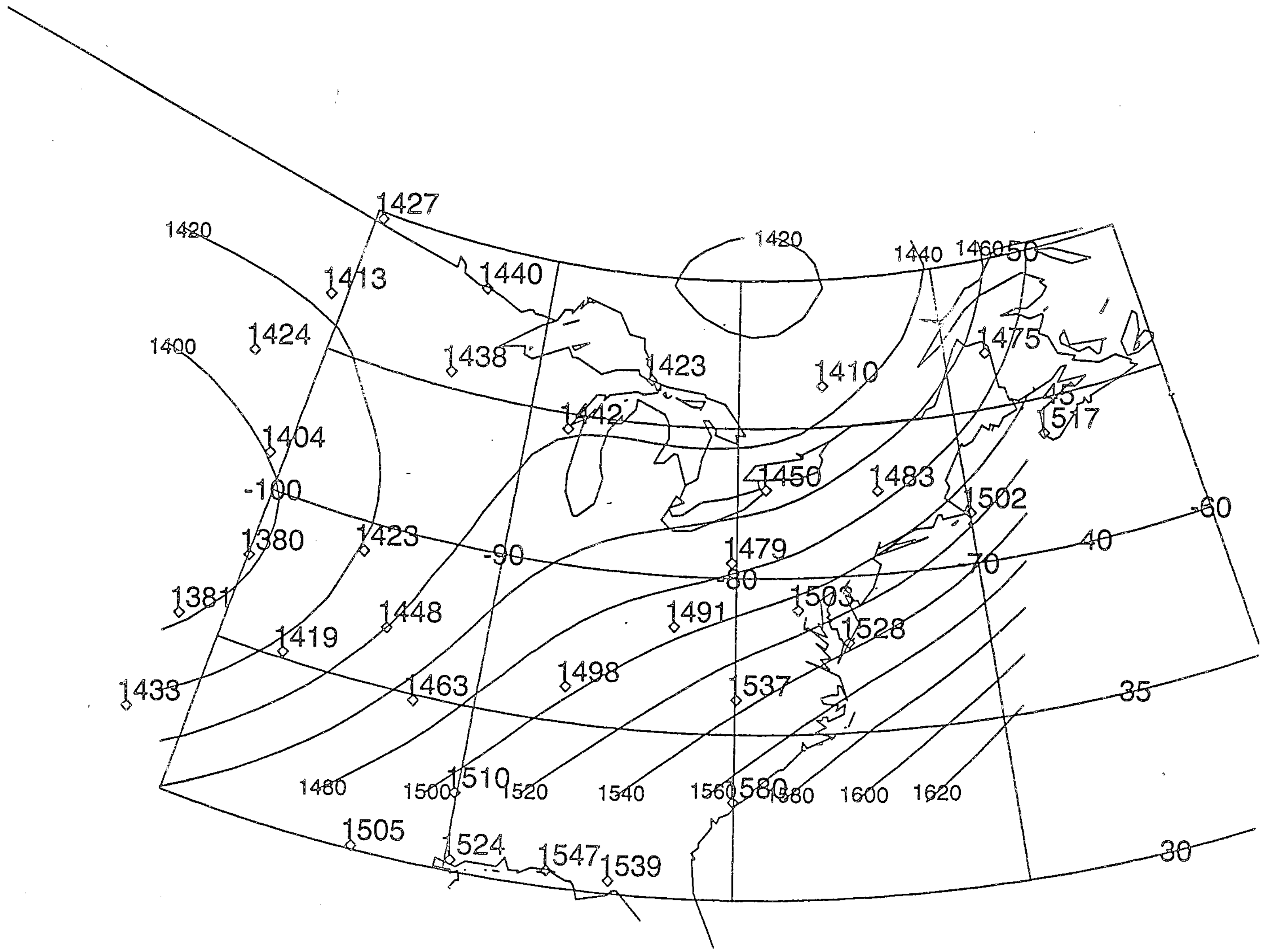

12 UTC 6 Mar 1995

Figure 7c

Analysis Increments

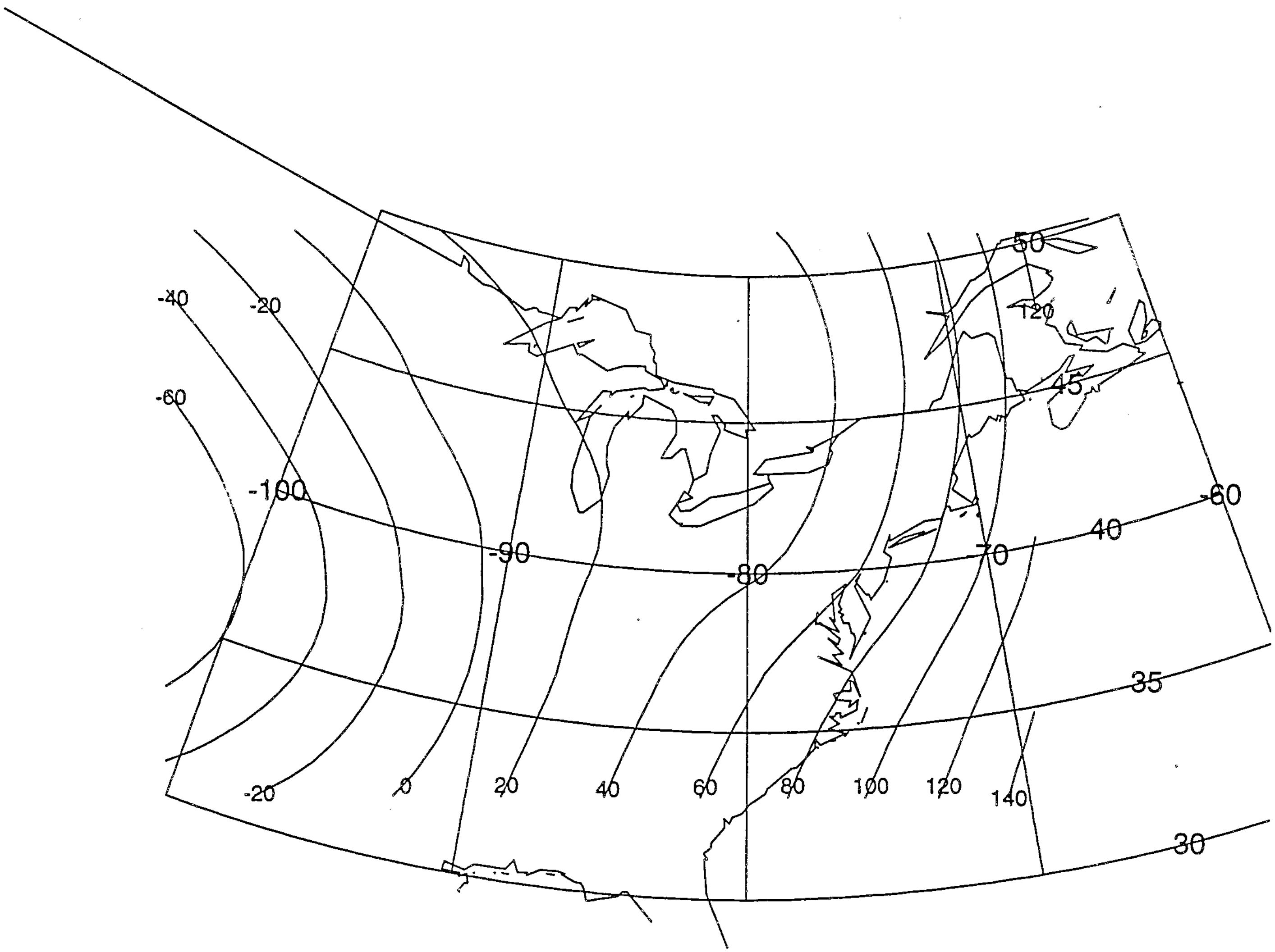

Figure 7d